Summer 2015

Myosin 10 is Required for Spinal Motor Axon Growth and Guidance in Zebrafish Embryos

Crystal Ivey

MYOSIN 10 IS REQUIRED FOR SPINAL MOTOR AXON GROWTH AND GUIDANCE IN ZEBRAFISH EMBRYOS

by

CRYSTAL IVEY

Under the Direction of Vinoth Sittaramane

ABSTRACT

Neurodevelopmental disorders are disabilities caused by malfunctioning mechanisms within the developing nervous tissue. These abnormalities often result in conditions such as autism spectrum disorders, Attention Deficient Hyperactivity Disorder (ADHD), motor dysfunctions, learning disabilities and mental retardation. Recent surveys indicate that there will be a 12% increase of children in the United States alone who are affected by neurodevelopmental disorders. Thus, it is important to understand both the normal and abnormal mechanisms of neural development. Neural development involves specification of new neurons and formation of neural circuits that connect the nervous system to every organ of the developing embryo. Neural circuits are formed by extensions of neuronal cell bodies called axons. Axons grow towards their specific target organs at growth cones, by sensing the environment for molecular cues which reorganizes their cytoskeleton to allow for their growth. Growth cones are actin rich suggesting that actin binding molecules play a vital role in axon guidance. Myosins are a class of actin binding proteins. *Myosin 10* (*myo10*) is a myosin that is highly localized in growth cones indicating their potential role in axon guidance and growth. While *myo10* has been shown to be involved in axon guidance in neural cell cultures, this has not been demonstrated *in vivo*. This aim of this project was to identify the roles of *myo10* in axon growth cone guidance *in vivo* utilizing a zebrafish (*Danio rerio*) model. I established that *myo10* is required for spinal motor and hindbrain axon development in the zebrafish. In the absence of *myo10*, 100% of caudal primary motor neurons were defective and 88% of middle primary motor axons were defective. Additionally, I characterized the phenotype of *myo10* deficient embryos further by examining the points of innervation of the motor axons. Spinal motor axons innervate the muscle. The post-synaptic muscle is lined with acetylcholine receptors. *Myo10* deficient embryos have a defective patterning of acetylcholine receptors and the muscles show indications of atrophy. Lastly, I provide some evidence for possible mechanisms in which *myo10* may be functioning.

INDEX WORDS: Growth cone, Axon Guidance, myosin 10

MYOSIN 10 IS REQUIRED FOR SPINAL MOTOR AXON GROWTH AND GUIDANCE IN ZEBRAFISH EMBRYOS

by

CRYSTAL IVEY

B.S., Georgia Southern University, 2013

A Thesis Submitted to the Graduate Faculty of Georgia Southern University in Partial Fulfillment of the Requirements for the Degree

MASTERS OF BIOLOGY

STATESBORO, GEORGIA

MYOSIN 10 IS REQUIRED FOR SPINAL MOTOR AXON GROWTH AND GUIDANCE

IN ZEBRAFISH EMBRYOS

by

CRYSTAL IVEY

Major Professor: Vinoth Sittaramane
Committee: John S. Harrison
Oscar Pung

Electronic Version Approved:
July 2015

TABLE OF CONTENTS

CHAPTER 1

INTRODUCTION

Purpose and Importance of the Study

This study aims to understand the roles *myo10*, a potential axon guidance molecule, plays in the process of neurodevelopment. Neurodevelopment is a critical process during embryogenesis that gives rise to the nervous system. In all vertebrates, the nervous system consists of the brain, spinal cord, and the nerves that exit the spinal cord and make synapses with various structures throughout the body. The schematic in Figure 1 displays the brain and the spinal cord in green and the spinal nerves that exit the spinal cord in blue. The cell body of each nerve is located in the spinal cord or brain and has a long protrution called an axon. During development, the axon of each cell body extends and projects away from the spinal cord to synapse with a specific collection of target cells. However, molecular deficits can lead to a failure of axons to migrate appropriately and fail to synapse with their targets (Ehninger et al 2008). Depending on the nature of the molecular deficiency, this can lead to a wide array of neurodevelopment disorders that can range from mild to fatal. Common conditions that are the result of these neurodevelopment disorders are autism spectrum disorders, ADHD, motor dysfunctions, learning disabilities, and mental retardation. Recent surveys indicate that neurodevelopment disorders are predicted to increase 12% by the

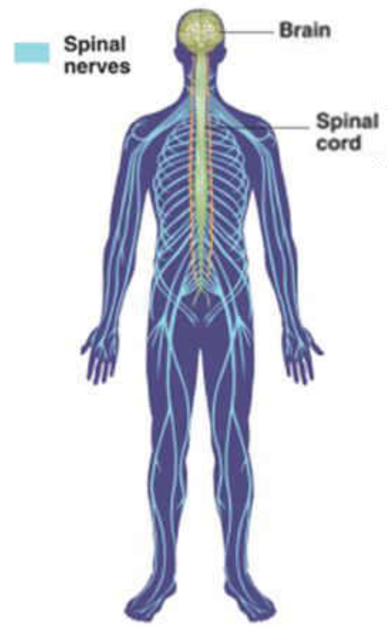

Figure 1. Schematic of the human nervous system. Picture amended from the McGraw Hill Company

year 2030 (WHO, 2007). These disorders have many possible causes such as nutritional deficiencies, injuries, exposure to toxins, maternal causes, and genetics. Susceptibility to neurodevelopmental disorders typically increase with age. As medical advances have been made over the past century, the life expectancy is on the rise. Thus, neurodevelopmental disorders are drastically increasing (Brown et al. 2005). These disorders have a huge impact on not only the patient, but also society as a whole. The overall economic cost of neurodevelopmental disorders in the United States is estimated to be $81.5–167 billion dollars per year (Szpir, 2006). Thus, it is important to understand both the normal and abnormal mechanisms of neural development. Some studies have used cultured cells to study axon guidance molecules *in vitro* (Yu et al. 2012). However, *in vivo* experimentation will give more insight on how proteins function in living systems. Others have demonstrated the use of model organisms such as frog,rat, mouse, chick, and fish to uncover the genetic abnormalities that cause neurodevelopment disorders in humans. For example, X.J. Zhu et al. 2007 used rats as model organisms to reveal that *myo10* has a role in axon path-finding. However, zebrafish have recently become a widely used tool in neurodevelopment research. Zebrafish have many attractive properties for research. Firstly, 70% of human genes have at least one zebrafish orthologue (Howe et al. 2013). Also, the reproductive capability of zebrafish is impressive. They can lay 150-200 embryos per week. This allows ample opportunity for experimentation. Additionally, the embryos are fertilized externally allowing for easy embryo collection and manipulation. Also, the embryos are transparent. This enables the use of protocols such as whole mount *in situ* and antibody labeling. Furthermore, the embryos undergo complete embryogenesis within 3 days making data collection very quick in comparison to other models. Finally, there is a plethora of information already known about zebrafish. Their genome has been sequenced and many studies have already utilized zebrafish resulting in databases of information and optimized techniques.

Because other studies have demonstrated that *myo10* defects result in decreased neurite outgrowth and filopodial projections *in vitro*, **I hypothesized that *myo10* is required for spinal motor axon growth cone guidance *in vivo***. Therefore, I used the spinal motor axons in the trunk of the zebrafish as a model to investigate the molecular mechanisms of *myo10* in the development of the zebrafish nervous system. Using both morpholino oligonucleotide (MO) gene knock down and genetic mutants, I found that *myo10* is required for proper development of both the spinal motor axons. *Myo10* deficient embryos have truncated caudal primary (CaP) and truncated or missing middle primary (MiP) spinal motor axons. Because I demonstrated that *myo10* is required for spinal motor axon growth **I questioned if spinal motor axon defects resulted in muscle atrophy.** I observed mispatterning of acetylcholine receptors that are found in neuromuscular junctions and a decrease in myofibril width. These results are indicative of muscular atrophy. Lastly**, I asked where *myo10* could be functioning.** Using both morpholino oligonucleotide (MO) gene knock down and genetic mutants I found that neural crest cell migration is partially arrested in the neural tube leading to less neural crest cells migrating. This provides evidence that *myop10* is functioning within the neural crest cells. If motor axon migration is dependent upon proper neural crest cell migration, then the faulty neural crest cell migration due to *myo10* deficiencies could indirectly result in axon guidance defects. Additionally, I used synthetic *myo10* mRNA to overexpress *myo10*. This yielded an increased number of protrusions along the CaP motor axon compared to controls. This provides evidence that *myo10* is functioning within the axons. I also observed defects in other areas where *myo10* is expressed. Commissural axons in the hindbrain do not form as a result of the *myo10* defect suggesting that *myo10* is specific to its expression pattern.

CHAPTER 2

THE BIOLOGY

2.1: Early Neural Development

In the early stages of vertebrate development, a series of rapid mitotic events results in a sheet of cells located on the dorsal part of the embryo that will form the components of the nervous system (Schmidt et al. 2013). This region is called the neuroectoderm. Within the neuroectoderm, a region of cells express certain genes that agonize the formation of the neural plate (Schmidt et al. 2013). Figure 2 chronologically demonstrates how the outer edges of this plate move toward one another to create an invagination (Nandadasa, et al. 2009) that ultimately continues until the outer edges come together and pinch off to form a tube-like structure that runs rostocaudally through the embryo and migrates away from the remaining dorsal ectoderm. This tube-like structure is known as the neural tube; it is the predecessor to the brain and spinal cord. As embryogenesis continues, cells within the neural tube generate axons that extend away from the neural tube. These axons will synapse with target cells.

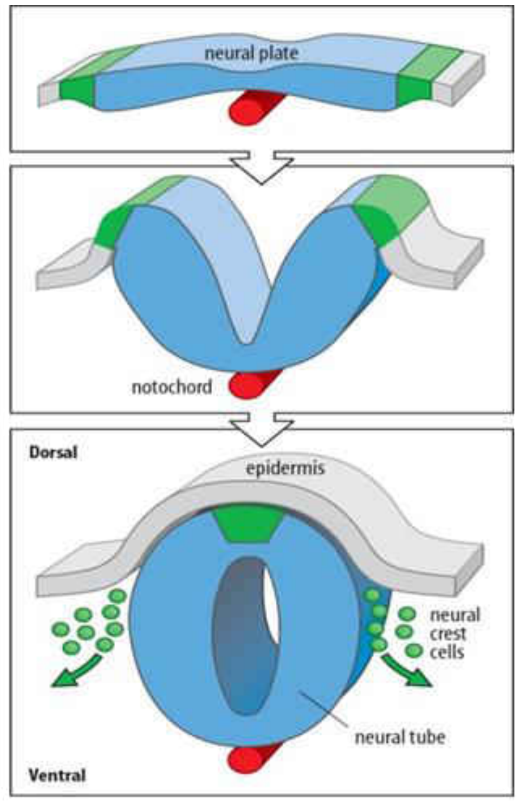

Figure 2. Neural plate folding to form the neural tube while neural crest cells migrate laterally. Picture from http://medchrome.com/wp-content/uploads/2010/11/neurulation.jpg

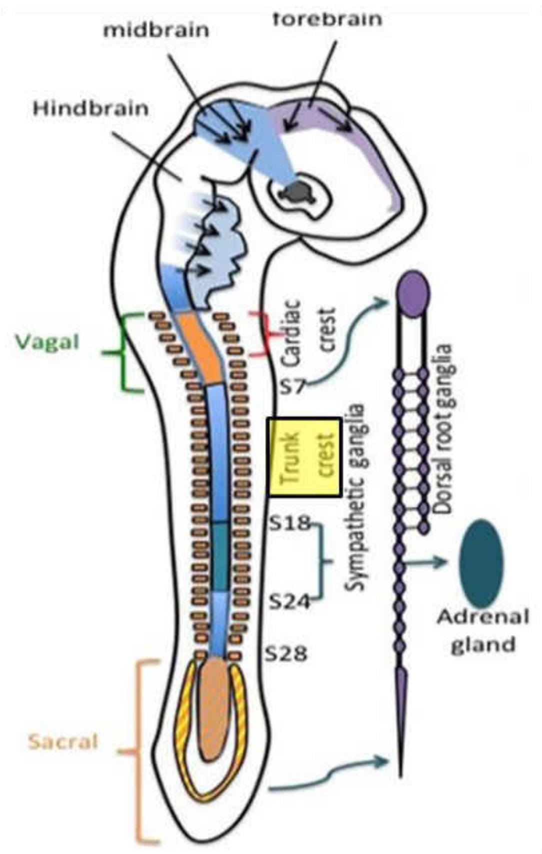

Figure 3. Neural crest cell specification during development. Picture amended from Pierdomenico Ruggeri et al. "Neurotrophin and Neurotrophin Receptor Involvement in Human Neuroblastoma" 2013.

In addition to axon formation and elongation at the neutral tube, another population of cells migrates away from the neural tube. These cells are known as neural crest cells (NCC). Neural crest cells are migratory cells that differentiate into several cell types that serve various functions depending on the location that they ultimately migrate to. Figure 3 shows the four domains that neural crest cells can be classified into: the cranial, trunk, cardiac, and the vagal/sacral neural crest cells (Mayor and Theveneau, 2013). Each neural crest cell type has a different function. The trunk neural crest cells that are highlighted in yellow in Figure 3 will go on to form the dorsal root ganglia for sensory neurons. During their migration, these neural crest cells are segmentally organized into streams (Banerjee, S et al. 2012). Interestingly, is has been demonstrated in frog that these neural crest cells migrate in a synchronous manner with axon migration (Banerjee, S et al. 2011).

2.2: Neural Circuitry and Specification of Axons in the Trunk

As mentioned before, the cell body of each neuron is located in the spinal cord while a long extention called the axon migrates to a collection of target cells. There are two main types of axons: primary and secondary axons. The proteins responsible for axon specifiication in the nerual tube are Sonic Hedgehog (*shh*) and Bone Morphogenic Proteins (BMPs). *Shh* and BMPs are morphogens that pattern tissue development (Avilés et al. 2013). Figure 4 A and B shows that *Shh* is secreted from a ventrally located mesodermal structure called the notochord and migrates to

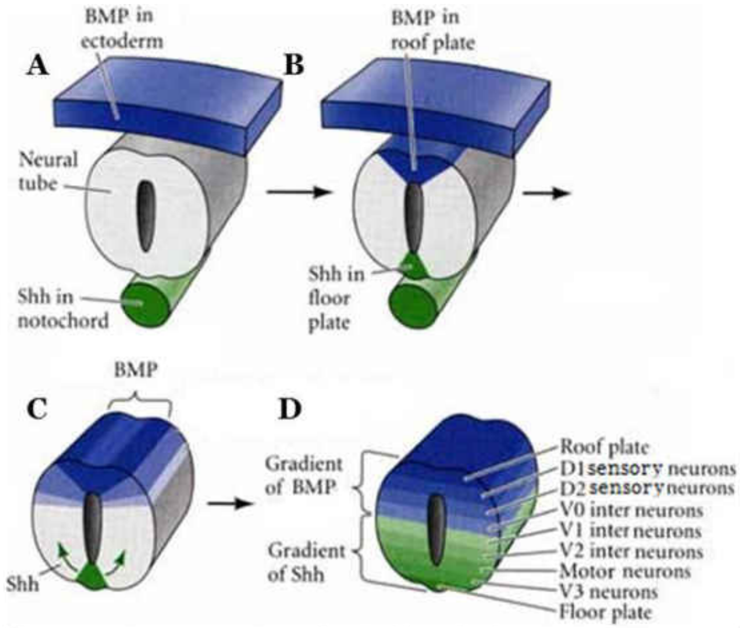

Figure 4. Cross section of neural tube showing inverse concentration gradients of *shh* and BMPs that result in neuron specification. Pictures amended from Gilbert, 2010.

the floor plate in the ventral portion of the neural tube while the ectoderm secretes BMPs that migrate into the roof plate in the most dorsal section of the neural tube (Charron and Tessier-Lavigne, 2007). BMP-dependent down-regulation of Shh causes result in the reciprocal concentration gradients of *shh* and BMPs (Bastida et al. 2009). Figure 4 C and D shows that these two concentration gradients within the neural tube cause specification of neurons. With the specific concentration of *shh* in the region of the neural tube labeled in Figure 4 D "motor

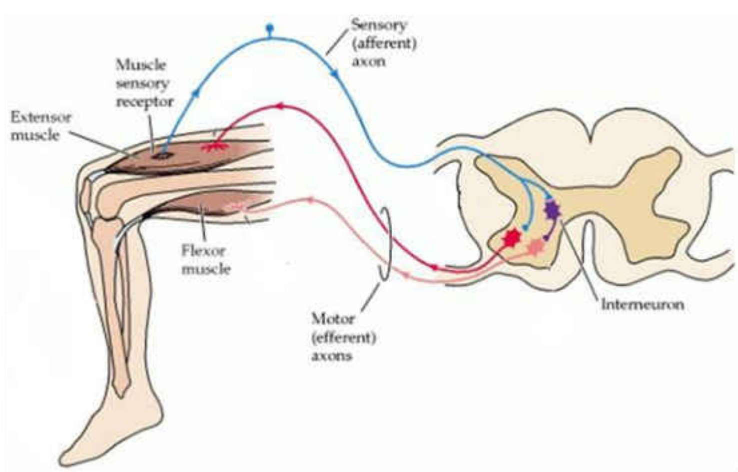

Figure 5. Neuromuscular Circuit schematic. Image amended from Purves et al. 2001

neurons", neurons become primary motor neurons. The remaining concentrations of *shh* and BMPs result in various other secondary neurons such as interneurons and sensory neurons. All of these neurons work together to complete a neural circuit. Figure 5 models a neural circuit that powers muscle movement. A neural circuit consists of a sensory neuron, an interneuron, and one or more primary motor neurons. Activation of a neural circuit results in excitement within the neuromuscular junction to perform an appropriate action based on the initial sensory signal (Eisen, 1991). The primary motor neurons in each of these neuromuscular circuits have the largest cell bodies, thicker axons, and exit the spinal cord very early (Bernhardt et al. 1990) in comparison to the remaining classes of neurons. Because of this, they are more easily examined and manipulated during experimentation and therefore were used for the duration of this study.

2.3: Primary Motor Axon Development and Morphology

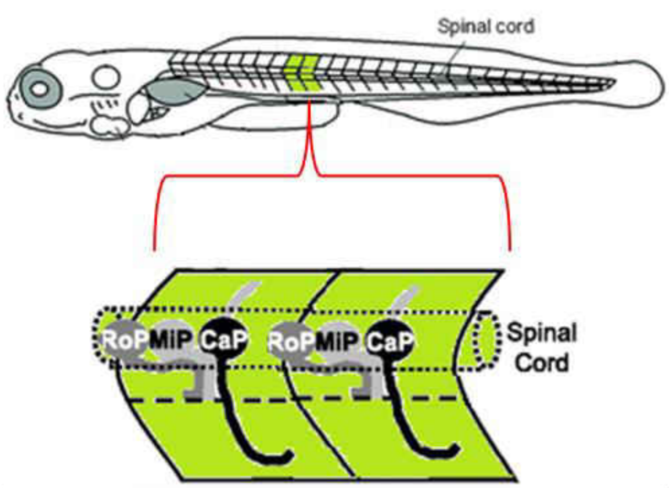

Figure 6. Schematic diagram of a zebrafish embryo displaying the segmentation pattern seen along the rosto-caudal axis and an enlarged section of two myotomes with one pair of their associated motor neurons each. Pictures amended from Sung-Kyun Ko et al. 2011 and Paola V. Plazas et al. 2013

The trunk of the zebrafish is divided into segments called myotomes. Figure 6 depicts the segmentation pattern of the myotomes and also shows that each myotome contains a set of three motor neuron cell bodies; the rostral primary, middle primary, and caudal primary cell bodies. The cell bodies generate a long protrusion called an axon (Hirokawa et al. 2010). This axon has a dynamic structure at the most distal tip called the growth cone (Bashaw and Klein, 2010). The growth cone is an extremely dynamic structure that contains a cytoskeletal network of microtubules along its shaft with a more distal population of microtubules that have not yet been stabilized (Dent et al. 2011). These unstable microtubules are encapsulated by the lamellipodia of the growth cone as well as the finger-like projections of the lamellipodia called filopodia. The lamelliapodia and filopodia are actin rich and are controlled by constant actin polymerization and degradation (Betz et al. 2009) that is dependent upon molecular cues in its periphery resulting in a reorganization of its cytoskeletal microtubules and thereby allowing for targeted growth (Roche et al. 2009). This process essentially "steers" the growth cone in the appropriate direction to guide the axon to its predetermined target. According to Ananthakrishnan and Ehrlicher (2007), neural outgrowth is carried out in three cyclical steps. Figure 7 gives a demonstration of this process. First, filopodia extend to explore the extracellular matrix (ECM) in search of molecular cues (A). In response to the detection of axon guidance molecules in the ECM, a new focal contact forms with the help of cell adhesion molecules that bind the new

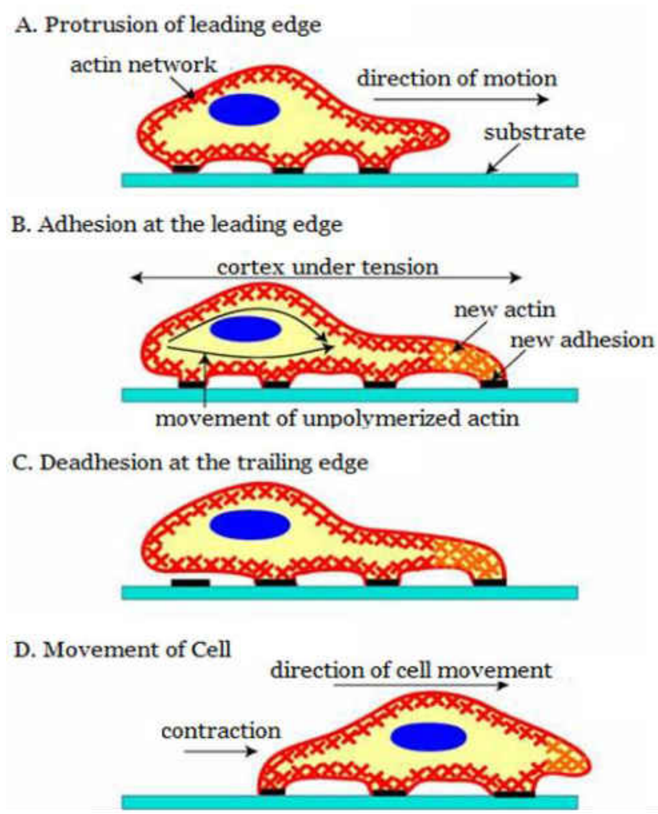

Figure 7. Model of cell migration. Picture amended from Ananthakrishnan and Ehrlicher, 2007.

filopodia to the extracellular substrate (B). The tail end of the cell will then release its trailing edge adhesive contact (C) and complex contractile forces then cause the trailing edge of the cell to move in the wake of the leading edge (D). Using this process, the three primary motor axons in each segment follow specific trajectories in an independently manor to extend to the first intermediate target seen in Figure 8 and then migrate in different directions; even when confronted identical environments (Pike and Eisen, 1990). The axons are named based on the direction that they project and their order of emergence. The CaP motor axon emerges from the spinal cord first and projects ventrally. The MiP motor axon emerges and projects dorsally. Lastly, the rostral primary motor neuron (RoP) emerges and projects laterally (Pike and Eisen, 1990). Axons often times must travel extremely long distances without error. Ablation experiments have demonstrated that this feat is simplified by breaking axon trajectories in to segments. As axons travel, there are “check points” where specialized cells ensure proper growth cone migration. These cells also present additional guidance information to initiate growth in the appropriate direction that will lead them in the direction of the next checkpoint until they synapse with their target. (Tessier-Lavigne and Goodman, 1996). This process has proven to be very complex; requiring a multitude of guidance molecules to work in a precise spatial

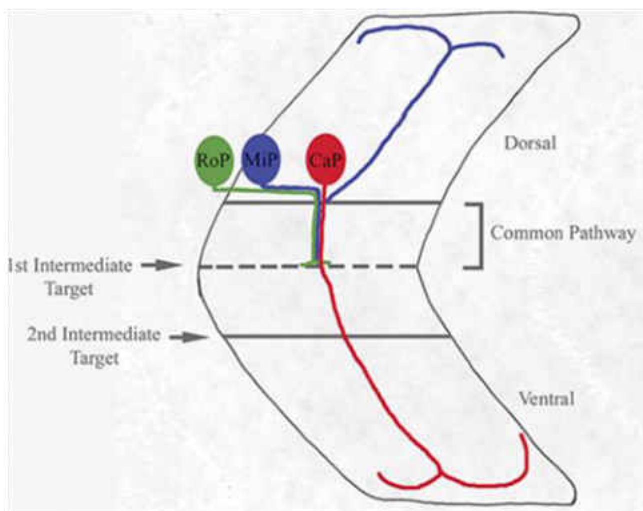

Figure 8. Routes traveled by each primary motor neuron in each segments of the zebrafish; the solid horizontal liens drawn outline the notochord. Picture amended from McWhorter et al. 2003

and temporal fashion in order to achieve proper neurulation throughout an organism. Previous studies have elucidated several molecules to be involved in this process.

2.4: Axon Development: Molecules

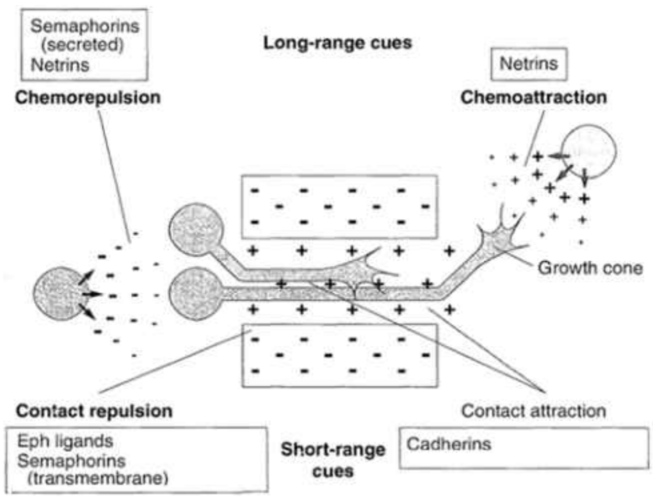

Figure 9. Summary of known axon guidance molecules. Picture amended from Tessier-Lavigne and Goodman, 1996.

As axons leave the spinal column and migrate to synapse their target cells, their sense of direction is obtained from molecular cues within the environment. The molecules contribute to axon guidance by interacting with the growth cone and can be categorized into two main groups; those that act on axons from a great distance (chemo group) and those that acts on axons from a short range (contact group). Each of these two groups is further subdivided into two additional groups; cues that attract and cues that repel (Tessier-Lavigne and Goodman, 1996). All in all, this divides molecules into four total groups; the chemo-attractants, chemo-repellants, contact attractants, and contact repellants (See Figure 9). The trajectories of each axon are believed to be dependent upon the simultaneous responses of a growth cone to all four types of molecular cues where long range cues act to guide the axon in a general direction and short range cues work to hone in on precise axon migration (Tessier-Lavigne and Goodman, 1996). Each axon in a developing embryo responds to molecular cues in the environment differently depending on the variable presence of receptors found on each growth cone (Winckler and Mellman, 2010) in conjunction with the extrinsic cues generated using mechanisms such as localized protein synthesis (Jung et al. 2013). All in all, these molecular cues coupled with receptors in a way "steer" the growth cone by promoting the initiation, extension, stabilization, or retraction of individual filopodia in specific regions of the growth cone (Dent et al. 2011). During the 1990s, several molecular cues and receptors were found to contribute to axon guidance *in vivo* (Dickson, 2002). Since then, a huge effort has been put forth to create a full view of the molecular mechanisms of axon development. While there is a noteworthy amount of information known about external molecular cues in the extracellular matrix, the amount known about molecules within the axons that drive axon guidance is lacking. It has been convincingly demonstrated that *myosin 2* (*myo2*) plays a role in axon guidance by controlling F-actin polymerization and retrograde flow within the axons (Lowery and Vactor, 2009). However, it is highly unlikely that *myo2* is the only axon guidance molecule that functions within the axons because this would not permit compensation if there was a defect in the *myo2* protein. Instead, it is a common phenomenon in living systems for multiple proteins to have functional redundancy. Functional redundancy allots a system multiple mechanisms to control a specific process. It is therefore likely that there are other contributors in the signaling pathways of axon guidance. Such contributors are most likely other molecules that can associate with actin (Dent et al. 2011) and regulate the retrograde flow of actin filaments (Dickson, 2002).

2.5: Myo10 and Axon Guidance

Myosins are divided into two types; conventional myosins (*myo2*/muscle myosins) and unconventional myosins; which are further subdivided into several other classes (Hasson et al. 1996). Recently, a novel unconventional myosin, *myo10*, has gained attention in our search for novel players in axon guidance. Figure 10 shows the hypothesized structure and molecular mechanism of the myosin 10 protein.

Structurally, all myosins contain three main domains; a head domain, a neck domain, and a tail domain. The head domain of myo10 binds to actin while hydrolyzing ATP to produce force. Myo10's neck domain functions in determining the progression of movement along actin filaments. Finally, the tail contains several subdomains that allows for dimerization, cargo carrying, and microtubule binding. With this structure, it is believed that myo10 dimers "walk" along actin filaments in a processive, hand over hand fashion where each myosin head alternates the lead progressing along actin filaments at about 34 nm per "step" (Qing Lu et al. 2011).

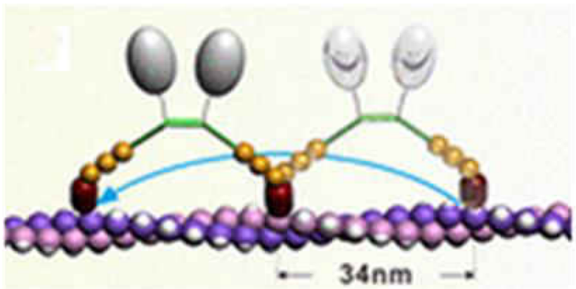

Figure 10. Unconventional myosin 10 dimer walking down actin filament in. (Qing Lu et al. 2012)

Preliminary data in Figure 11 shows that *myo10* is concentrated in the dorsal part of the spinal cord at 18 hours post fertilization (hpf) and is continuously present in migrating axons through at least 30 hpf in zebrafish. *Myo2*, which has already been established as an axon guidance molecule has a similar expression pattern; where it is concentrated in the central nervous system during early embryonic development and expands to other organs as embryogenesis continues (Huang et al. 2013).

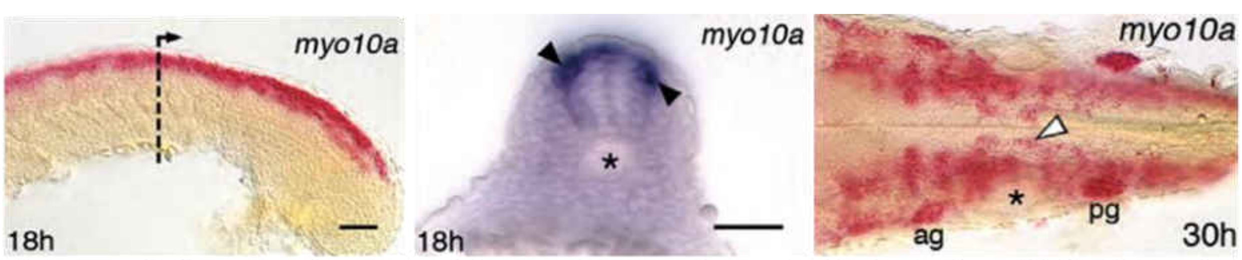

Figure 11. Left: myo10a is expressed in a continuous column of cells in the dorsal half of the spinal cord 18hpf. Middle: myo10a is expressed in migrating neurons (black arrows) 18 hpf. Right: Expression patterns of myosin 10a 30 hpf persists in the sensory ganglia and migrating motor neurons (arrowhead); ag/pg, anterior and posterior lateral line ganglion. Photos amended from Sittaramane and Chandrasekhar, 2008.

There are several possible mechanisms in which *myo10* deficiencies could cause axon guidance defects. *Myo10* could reside within the axons acting as a molecule involved in actin polymerization or microtubule stabilization. Also possible is that *myo10* plays a role in neural crest cell migration that ultimately causes a secondary effect on axon guidance. Here I used zebrafish as a model organism to study the roles that *myo10* plays in axon guidance.

Chapter 3

MATERIALS AND METHODS

3.1: Fish Lines and Embryo Collection

Adult zebrafish were all maintained or raised in a laboratory system following the published methods of Westerfield, 2007. The stages of development throughout this project were denoted in hours or days post fertilization according to a published staging series (Kimmel et al., 1995). An IUCAC proposal was submitted and approved for all research done in our lab using live zebrafish. I received all zebrafish from the Zebrafish Mutation Project. While most of the experiments done were on "wildtype" non-transgenic zebrafish, I also used the following transgenic lines: Ptf1a, mnx-1, and isl1. Transgenic Mnx-1 [Tg(*mnx-1:GFP)*] uses the mnx-1 promoter to drive the production of the Green Fluorescent Protein (GFP) within the cells that produce mnx-1 proteins; mainly the primary motor neurons. Thus, Tg(*mnx-1:GFP*) zebrafish will fluoresce motor neurons in green. Tg(*Ptf1a:GFP*) expresses GFP in the pancreas and cerebellum.

Tg(*isl1:GFP*) drives GFP expression in cranial motor neurons. During the immunohistochemistry antibody labeling protocol, fish were fixed in 4% paraformaldehyde. This process washes away the green fluorescent protein. Therefore, virtually any transgenic line can be used for antibody labeling as long as the transgenic GFP is removed.

Adult fish were removed from their living quarters and placed into smaller breeding tanks overnight. The males and females were separated by a plastic screen until approximately 9:00 am. Once the males and females were allowed to socialize amongst each other and the fertilization process ensued, embryos were collected and placed in a petri dish with E3 zebrafish medium and stored in an incubator (28°C). All embryos had their medium replaced twice daily for the extent of the experiment to prevent toxicity buildup and death. In order to enhance visibility, all embryos were exposed to 50µl of 1-phenyl 2-thiourea (PTU, 0.003% final concentration) per petri dish at approximately 16 hpf to prevent pigmentation. Once the embryos reached the appropriate age for the particular experiment, they were dechorionated, fixed in 4% paraformaldehyde, and sored at 4° C.

3.2: Obtaining Morphants and Mutants

Axon development was characterized by comparing control zebrafish larvae to *myo10* morphants or genetic mutants. In order to create *myo10* morphants I utilized a MO based knockdown. MOs are laboratory synthesized RNAs that are typically around 25 base pairs long and are created to selectively attach to the mRNA of a gene of interest based on the rules of complementation (Bill, B. et al 2009). Additionally, MOs contain non-ionic phosphorodiamidate inter-subunit linkages that replace the traditional anionic phosphodiester linkages found in RNA backbone eliminating the negative charge. Taken together, the addition of a complementary strand of nucleotides to the target mRNA creates a physical barrier that does not allow for the association of the mRNA with ribosomes while the neutral charge prevents association with nucleic acid binding protein. This provides a stable RNA structure with resistance to nucleases while still resembling natural nucleic acids (Summerton and Weller, 1997). In zebrafish, MOs are injected into the yolk of the embryos at the 1-8 cell stage to prevent disruption of the early blastomere(s). These blastomeres contain cytoplasmic bridges between them that allow for rapid diffusion of the MO throughout all of the cells (Bill, B. et al 2009).

To further corroborate the findings, I also utilized genetic mutants in experimentation. These genetic mutants were obtained from the Zebrafish Mutation Project. The Zebrafish Mutation Project subjects normal zebrafish to N-ethyl-N-nitrosourea (ENU) exposure (Kettleborough et al. 2013). ENU is a mutagen that causes random point mutations within the genomic DNA. ENU exposed sperm were collected and used to fertilize eggs generating heterozygous zebrafish. Because most of the zebrafish genome follows basic Mendelian Inheritance laws, crossing these heterozygotes with wildtype fish yields approximately 25% of the offspring that are homozygous for the mutation. The DNA of these fish were sequenced to identify where the mutation is. The zebrafish strain used in this project was sa728ix which has a nonsense point mutation within the *myo10* gene. Once a point mutation was confirmed within the gene responsible for the myo10 protein, offspring from the companies known heterozygotes were bought. The offspring consisted of a mixture of wildtype, heterozygous and mutant individuals. Once fully mature, they were crossed amongst each other. Observing the ratios of their offspring that had mutant phenotypes allowed me to identify which fish were heterozygotes. If approximately 20% of the embryos had morphant morphology, the parents were identified as heterozygotes. The whole embryo morphology used to detect genetic mutants is a dorsal curvature of the trunk.

3.3: Microinjections

Microinjections allow substances such as solutions, MOs, or extra-organismal cells to be introduced into a developing embryo. Embryos were collected using a mesh net. Some of these embryos were put aside during each experiment to serve as non-injected controls. The remaining embryos were microinjected with either *myo10* MO (Gene Tools Llc.), a control MO (Gene Tools Llc.), or co-injected with *myo10* MO and synthetic *myo10* mRNA (Ensembl ID: ENSDART00000113347) at the 1-2 cell stage. The *myo10* MO and control MO sequence is 5'CCTCTGCGAAGAAGGTCTCCATCTT3' and 5' CCTCTTACCTCAGTTACAATTTATA-3' respectively. The synthetic myo10 mRNA was synthesized and cloned into the pcs2+ vector by Genscript. Glass needles for injections were made using a 3.5" Drummond replacement tubes (#3-000-203-g/x) in a Model P-1000 Fleming/Brown Micropipette Puller. These needles were filled with 5 microliters of *myo10* MO diluted in phenol red and nuclease free water to generate a final, optimized concentration of 2 μg/μl. Once the *myo10* MO solution was in the needle, the needle was filled the remainder of its length with oil to eliminate any air. A small pair of micro tweezers were used to break the tip of the needle and allow passage of the *myo10* MO solution. To inject the *myo10* MO into the embryos, I used a Nanoject II™ Auto-Nanoliter Injector. Approximately 4.6 nanoliters of the *myo10* MO solution was injected into the yolk of each experimental embryo resulting in 9.2 ng of *myo10* MO. Rescue experiments were performed by co-injecting both *myo10* MO and synthetic *myo10* RNA at the 1-2 cell stage. When embryos reached the appropriate age for each experiment, they were manually dechorionated and fixed in 4% paraformaldehyde and stored at 4^{o} Celsius.

3.4: Immunohistochemistry

Znp-1, sox-10, F59, zn-8, and alpha-bungarotoxin (α-Btx) staining are common techniques applied throughout this experiment. All of these are antibodies with the exception of α-Btx which is a toxin derived from snake venom conjugated to alexa fluor 647 and purchased from Life Technologies. The alexa fluor conjugate has a fluorescent tag that enables the experimenter to visualize acetylcholine localization using fluorescent microscopy. All others are primary antibodies raised in either mouse or rabbit. Primary antibodies are made to recognize and bind to a pre-determined antigen. Secondary antibodies have florescent conjugates that bind to the primary antibodies and thus allow for the use of florescent microscopy to view a desired tissue, structure, or receptor, etc… Table 1 lists each antibody and concentration used.

Table 1. Antibodies Used for Immunohistochemistry Procedures

Primary Antibodies	**Concentration**
Znp-1	1:100
Sox10	1.5:100
F59	1:10
Zn-8	1:10
Secondary Antibodies	**Concentration**
Goat anti-mouse alexa fluor 488	2:500
goat-anti rabbit alexa fluor 568	2:500

I stained primary motor axons using anti-synaptogamin-2 antibodies (Znp-1, monoclonal, mouse, Zebrafish International Resource Center (ZIRC)). Muscles were stained using anti-myosin heavy chain antibodies (F59, monoclonal, mouse, ZIRC), neural crest cells were stained using anti-sox10 antibodies (sox-10, polyclonal, rabbit, GeneTex), hindbrain axons were stained using anti-neurolin antibody (zn-8, monoclonal, mouse, ZIRC). A secondary antibody raised in goat was introduced into the organism that recognizes antibodies of the species that the primary antibody was derived from. Primary antibodies raised in mouse were exposed to goat anti-mouse alexa fluor 488 (Life technologies) and primary antibodies raised in rabbit were exposed to goat-anti rabbit alexa fluor 568. This secondary antibody has a fluorescent tag. Thus, fluorescing the tissue in question.

Embryo antibody labeling was done using the same general protocol unless alpha-bungaroxoin was used. Alpha-bungarotoxin stains were washed in Incubation Buffer (IB) overnight before continuing with the general protocol. The general protocol included many washes in IB. The IB recipe contained the solvents DMSO and water. 1x Phosphate Buffered Saline (PBS) was sued as a buffer to keep tissues at normal pH levels. Triton x-100 acted as a detergent to permeate the tissue. This allowed antibodies that were later introduced to easily saturate the tissue. The formula also contained bovine serum albumin and horse serum that blocked non-specific binding of antibodies. Details of final concentrations of reagents for IB can be found in Table 2.

The general protocol is as follows:

Embryos were washed 4 times (30 minutes) in IB solution in 0.5ml tubes. After 4 washes of IB, the embryos will be washed in an additional solution of IB containing 1% horse serum (500 µl IB + 5µl horse serum). The horse serum also blocks non-specific binding of antibodies. Afterwards, primary antibodies will be added to a solution of IB with 1% horse serum and allowed to incubate overnight (1:100 dilution of znp-1, 1:10 dilution of Zn-8 and F59, and 1.5:100 dilution of sox10). If alpha-bungaroxtin was used, the embryo (which has already been in IB overnight) was washed with IB and horse serum for 30 minutes. Another was done afterwards with IB, horse serum, and a 1:500 dilution of alpha-bungarotoxin. After 30 minutes, any additional primary antibodies were added and left to incubate overnight.

The embryos received an additional set of 4 washes for 30 minutes each of IB the following morning. Afterwards, they were washed in a solution of IB and 1% horse serum and then incubated overnight in IB, horse serum, and the appropriate secondary antibody (2:500 dilutions). All embryos except those stained with alpha-bungarotoxin were then incubated overnight in 4% paraformaldehyde/1XPBS (PFA in PBS). Alpha-bungarotoxin stains were immediately mounted. To mount the embryos on a slide, they were washed 3 times in 1xPBS for 5 – 10 minutes and then moved into a 24-well plate and washed in a 25% solution of glycerol. Once the embryos sank to the bottom (~10 minutes), they were washed with 50% glycerol for 10 minutes. Afterwards they will be placed into a 70% glycerol solution. Once in the 70% glycerol solution, individual embryos were placed on slides and decapitated with micro scissors. The trunk will be oriented laying on its side with its caudal end pointed left and rostral end pointed right. Small globs of Vaseline will be placed at the edges of the slide in a square pattern in such a way that each corner of a coverslip placed over the embryo would touch the Vaseline. The coverslip will then be secured by the Vaseline and the slide ready for examination.

Table 2. Reagents and Final Concentrations for IB	
50 ml IB	
Reagent	**Final Concentration**
25 ml 2xPBS	1x
23 ml dH_2O	--
500 mg Bovine Serum Albumin	1%(w/v)
1.5 ml TritonX100	3%(v/v)
.5 ml DMSO	1%(v/v)

3.5 Software and Statistical Analysis

Confocal imaging was performed using ZEN 2011 or 2012 software on a LSM 710 confocal microscope. The trunks of zebrafish were mounted laterally with anterior to the right and posterior end to the left. Slides were mounted onto the microscope face down. This inversion caused the images to display with the anterior end to the left and posterior end to the right at the time of image acquisition. Images were taken in z-stacks; 3D. Approximately 20 slices were images per picture. All test performed were statistically analyzed by either a students' T-test or G-test using JMP Pro 10 software. Students' T tests were used when analyzing averages of neural crest cells. All other statistics performed were of percentages which were analyzed using the G-test. Each conclusion was drawn from a minimum of 3 experiments using *myo10* MO injected embryos and 1 of genetic mutants unless otherwise denoted in graphs. Each experiment observed phenotypes from at least 5 embryos. 3 myotomes were observed per embryo each time.

Chapter 4

RESULTS

4.1 *Myo10* is Required for Spinal Motor Axon Growth and Guidance

4.12 *Myo10* Deficiency Results in Spinal Motor Axon Defects

In order to test roles that *myo10* has on zebrafish neurodevelopment, morphological phenotypes of Control and myo10 deficient embryos were compared. Figure 12 shows a side by side comparison of each group's trunk. The morphants consistently have defected trunks. Most trunks formed, but were extremely crooked while some did not appear to form at all. All morphants had mobility defects. Because

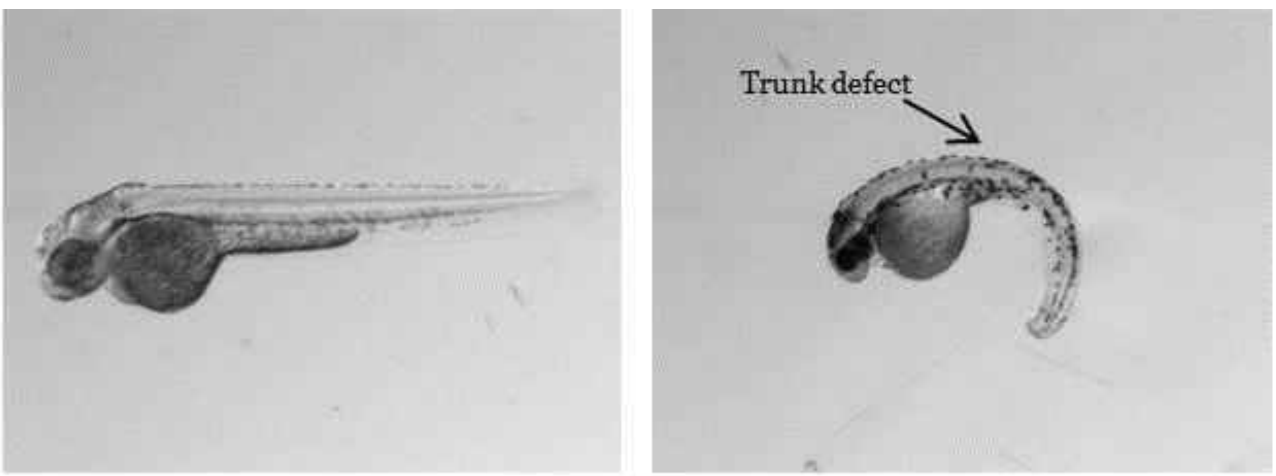

Figure 12. Whole embryo morphology of 48hpf control (left) and *myo10* morphant (right) embryos. Morphants have defected trunks that do not form straight and sometimes do not form at all. Images taken at 20x.

zebrafish have transparent embryos, I was able to utilize antibody staining techniques to fluorescently label the primary motor axons in the zebrafish larvae. Figure 13 shows a schematic of a zebrafish embryo with an enlarged schematic of 3 myotomes of the zebrafish embryo. Each embryo was viewed at 40x magnification to analyze the neural tissue of the CaP and MiP motor axons using a confocal fluorescent microscope. I observed a consistent stunt of CaP axon growth in *myo10* deficient embryos. Figure 13 displays a graphical representation of this data.

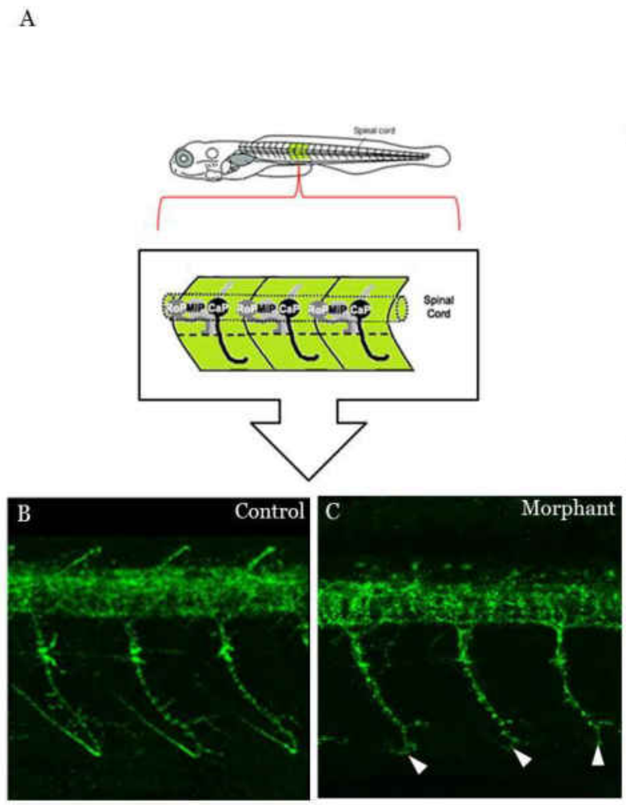

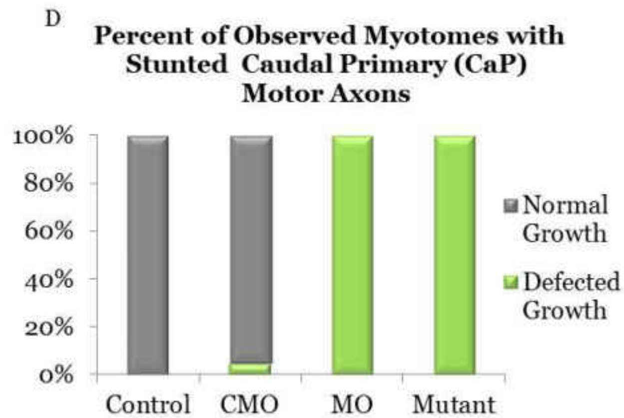

Figure 13. A: Schematic of zebrafish embryo with enlarge section of the 15^{th} – 17^{th} myotome. B, C: Confocal images of motor axons in 15^{th}-17^{th} myotomes of control (B) and myo10 MO-injected (C) zebrafish embryos at 48hpf stained with znp-1 antibodies. White arrows indicate truncated CaP axons. D: Summary of the Percentage of observed myotomes with stunted CaP axons in Control, Control MO-injected (CMO), MO-injected (MO), and genetic mutant embryos. $G = 151.95$, $DF = 3$, $p<.0001$, $n=118$; $G_{Control,\ CMO} = 1.58$, $DF = 1$, $p=.21$, $n = 50$; $G_{Morphant,\ Mutant} = 0.0$, $DF = 1$, $p = 1.0$, $n = 68$

MiP motor axons were also defective. Each embryo was viewed at either 20x or 40x magnification to analyze the percentage of defective MiP motor axons. Figure 14 displays a graphical representation of this data.

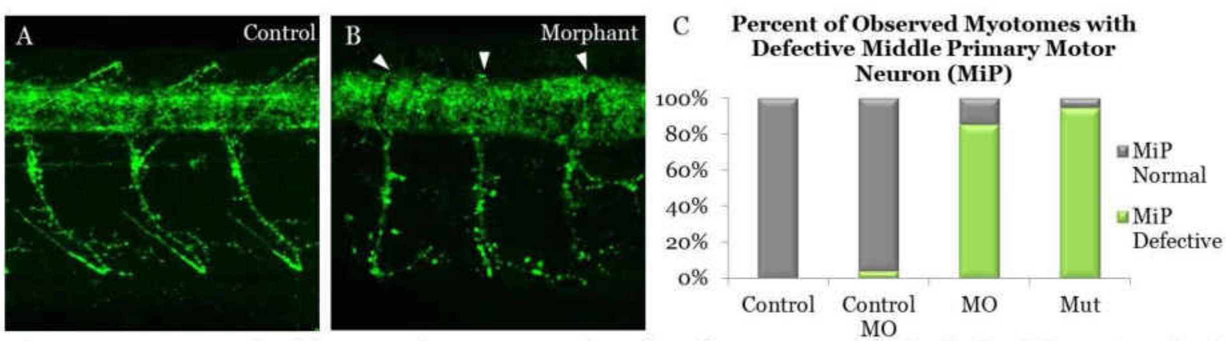

Figure 14. A,B: Confocal images of motor axons in 15^{th}- 17^{th} myotomes of 48hpf zebrafish trunk stained with znp-1 antibodies displaying (A) normal and (B) *myo10* MO–injected embryos. White arrows indicate missing MiP axons. C: Summary of the Percentage of myotomes observed with missing MiP axons. $G = 105.69$, $DF = 3$, $p<.0001$, $n=121$; $G_{Control,\ CMO} = 1.68$, $DF = 1$, $p=.19$, $n = 48$; $G_{Morphant,\ Mutant} = 1.174$, $DF = 1$, $p = .28$, $n = 73$

4.13 Spinal Motor Axon Defects Results in Defective Acetylcholine Receptor Patterning

Because the spinal motor axons of *myo10* deficient embryos do not extend as far as controls, I speculated that the spinal motor axons were not able to innervate the muscles. Innervation of the muscle by an axon is called a neuromuscular junction. Within these junctions are acetylcholine receptors on the muscle cell membrane that bind with acetylcholine that is produced by the pre-synaptic axon. By taking advantage of immunolabeling the acetylcholine receptors with α-btx in conjunction with the spinal motor axons with znp-1, I was able to view both the pre- and post-synaptic complexes of the neuromuscular junction. I hypothesized that the acetylcholine receptors would form normally while the axons would be truncated. Thus, revealing that the spinal motor axons would in fact be unable to make the connections in the distant neuromuscular junctions. However, as demonstrated in Figure 15, acetylcholine receptors remained closely co-localized with the spinal motor axons and did not extend into the muscle past the locations occupied by the spinal motor axons. Moreover, the acetylcholine receptors in *myo10* deficient were disorganized when compared to the controls; instead of a streamline flow of acetylcholine receptors, the acetylcholine receptors appeared blotchy.

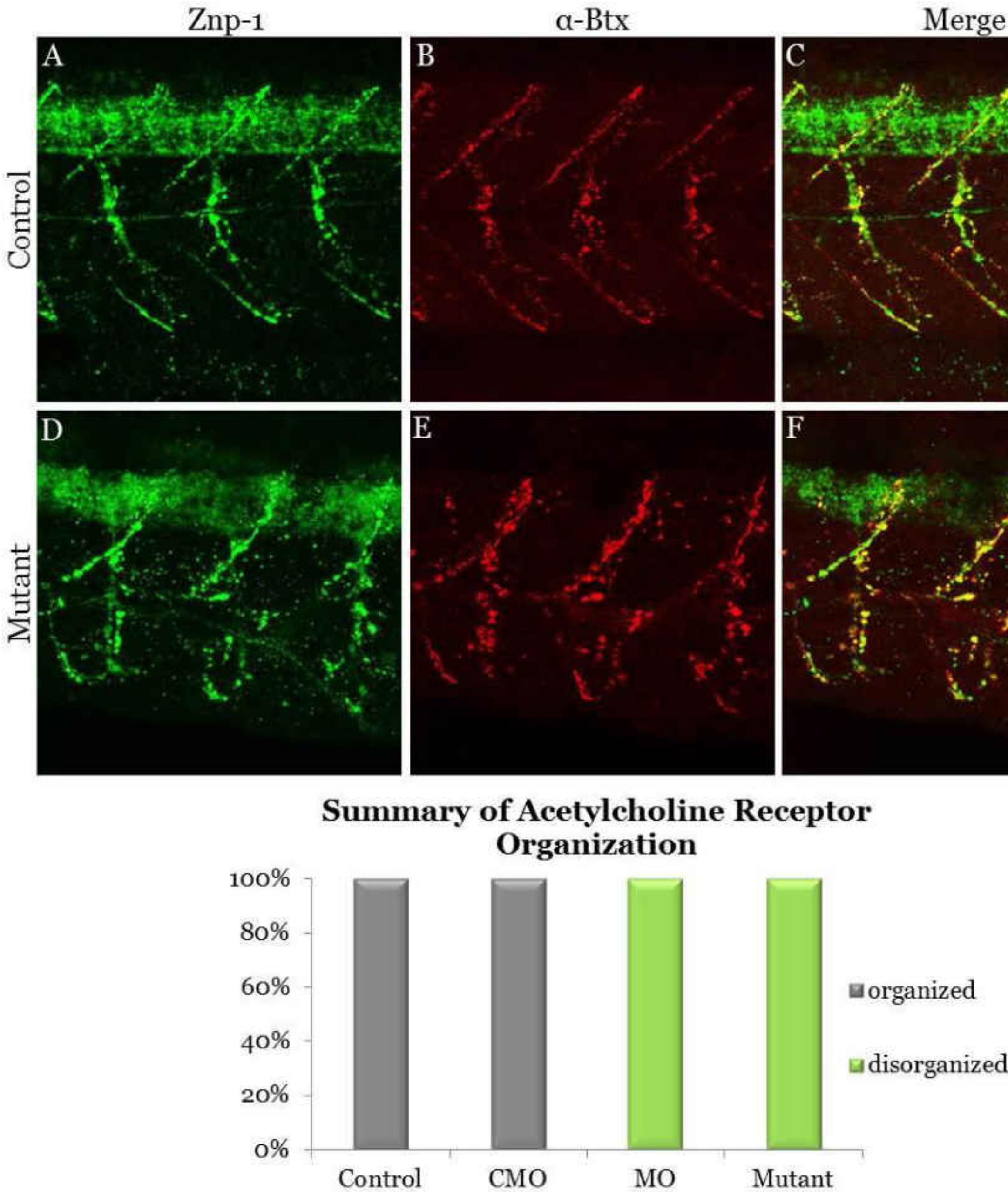

Figure 15. Confocal images of 15^{th}- 17^{th} myotomes of 48 hpf zebrafish trunks fluorescing the motor axons in green with znp-1 antibodies (A and D), the acetylcholine rectors in red with α-Bungarotoxin (B and E), and merged images of the motor axon and α-Bungarotoxin stains (C and F). Images reveal that *myo10* deficient embryos have a disorganized patterning of nicotinic acetylcholine receptors, while being highly co-localized with axon patterning. H: Summary of the organization patterns of control and myo10 MO injected zebrafish embryos. $G = 158.60$, $DF = 3$, $p<.0001$, $n=116$; $G_{Control, CMO} = 0.0$, $DF = 1$, $p=1$, $n = 50$; $G_{Morphant, Mutant} = 0.0$, $DF = 1$, $p = 1$, $n = 66$

4.14 Axon Defects Results in Muscle Defects

To further explore the possible roles that *myo10* plays in axon growth and guidance, I investigated the points of innervation for the spinal motor axons; the muscles. Muscles are derived from segmented paraxial mesoderm (Bassett and Currie, 2003) which in turn give rise to the myotomes. Once the muscles are formed, there are two different classes of muscle fibers; slow muscles and fast fibers. The two muscles types are topographically separable in the embryonic myotome as demonstrated in Figure 16. Slow muscles are located

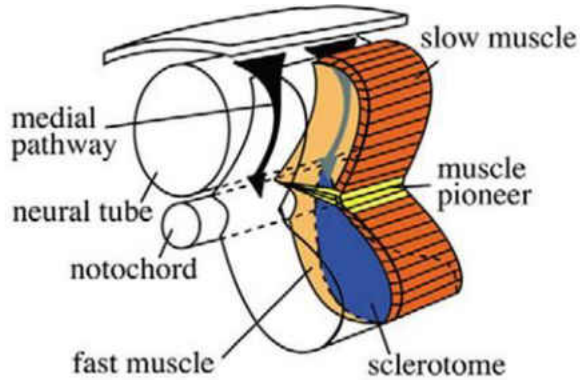

Figure 16. Schematic of a single zebrafish myotome. Slow muscle tissue (red) is located superficially in relation to the underlying smooth muscle (orange).

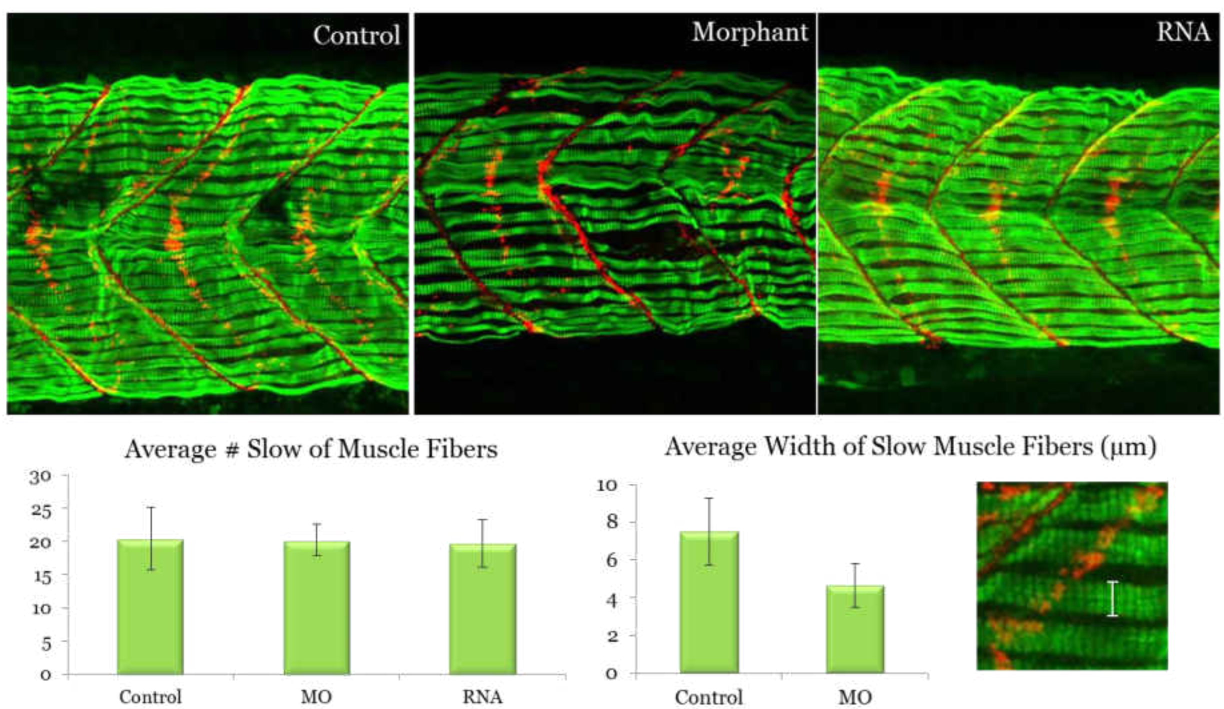

Figure 17. Confocal Images of 36hpf zebrafish trunk displaying alpha-bungarotoxin in red and muscle fibers in green using F59 antibodies. There is no significant difference in the number of muscle fibers per myotome between control, MO injected, or overexpressed muscles. One way Anova: DF = 2, F = .1481, p =.8628. However, morphant embryos have significantly smaller muscle fiber width than controls. Students T test: P<.0001

superficially and the fast muscles are located more medially within the embryo (Bassett and Currie, 2004). Figure 17 displays slow muscle fibers using f59 antibodies (green) and the acetylcholine receptors using alpha-bungarotoxin in red. Figure 17 explains that all groups have an equal number of slow muscle fibers per myotome. However, morphant individuals have a significantly decreased slow muscle fiber width. Calculations were made by measuring the width of four myofibrils per myotome. Two were measured immediately above and below the horizontal myoseptum pictured in yellow as “muscle pioneer” cells in Figure 16.

4.15 *Myo10* Defects Cause Axon Defects in the Hindbrain

In order to determine the specificity of *myo10* defect, I examined the commissural axons in the hindbrain. Commissural axons normally form and decussate at rhombomere boundaries (Riley et al. 2004) in the hindbrain. *Myo10* expression has been recorded at varying levels in rhombomeres 2–5 at 18hpf. *Myo10* expression continues in the hindbrain at 30hpf in the sensory ganglia and growing motor axons (Sittaramane and Chandrasekhar, 2008). Figure 18 demonstrates control, *myo10* MO-injected, and overexpressed 36hpf zebrafish hindbrains with zn-8 antibodies to observe the commissural axons. I saw that control and *myo10* overexpressed embryos form commissural axons normally; while the morphant individual’s commissural axons fail to form at all. Because there are defects in both the hindbrain axons and the spinal motor axons where *myo10* expression has been recorded previously, it is likely that *myo10* defects are specific to its expression pattern.

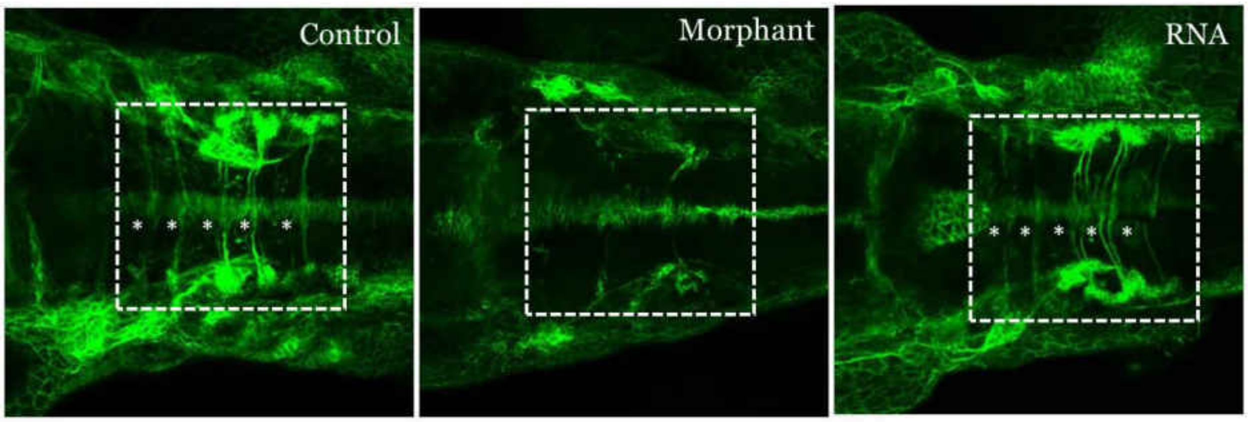

Figure 18. Confocal Images of 36hpf zebrafish embryo hindbrain displaying the commissural axons using zn-8 antibodies. White asterisk indicates individual commissural axons. Morphant embryos are missing these axons. Commissural axons are present in control embryos as well as in individuals injected with exogenous RNA. $G = 49.65$, $DF = 2$, $p<.0001$, $n=39$; $G_{Control, MO} = 36.04$, $DF = 1$, $p<.0001$, $n = 26$

4.2 Mechanisms Underlying the Role of *Myo10*

I have demonstrated that axon migration if affected by deficiencies of *myo10* in the spinal motor axons in the trunk and commissural hindbrain. However, the underlying mechanisms of how *myo10* function in this process are still obscure. The first step to understanding how *myo10* is functioning is to determine where it is functioning. Based on previously shown expression patterns (Sittaramane and Chandrasekhar, 2008), *myo10* is likely functioning within the axons themselves. Another possibility is that *myo10* is functioning within neural crest cells. Neural crest cell in the trunk delaminate from the spinal cord and migrate ventrally in segmentally constricted lines that migrate in a synchronous manner with spinal motor axons (Banerjee et al. 2013). It is possible that proper axon migration is dependent upon proper neural crest cell migration. If this is true, faulty neural crest cell migration due to *myo10* deficiencies would cause a domino effect on spinal motor axons. A final possibility is that *myo10* is functioning within both neural crest cells and spinal motor axons and that proper migration of the two cell types are caused by interactions between one another.

4.21 *Myo10* Plays a Role in Neural Crest Cell Migration

Myo10 has been demonstrated to be required for cranial and trunk neural crest cell migration in *Xenopus laevis* (Hwang et al. 2009). Disrupting *myo10* expression yields faulty neural crest migration where neural crest cells migrate shorter distances than normal embryos and also fail to migrate in the distinct streams seen in each hemisegment of the zebrafish embryo (Nie et al. 2009). While there previously was no demonstration of this data *in vivo* of the zebrafish trunk yet, other experiments in our lab have shown that neural crest cells are required for cranial neural crest cell migration in zebrafish. Preliminary data shown in Figure 19 provides evidence that *myo10* is also required for neural crest cell migration in the trunk. Control and morphant embryos were stained in green for spinal motor axons and in red for neural crest cell. To determine if there were neural crest migration defects, the bottom of the spinal cord was labeled with a dashed white line. Each neural crest cell above that line was categorized as “dorsal” and each neural crest cell below the white line was categorized as “ventral”. The number of the neural crest cells in each category was counted manually by viewing slice by slice of a z-stack in zen2012 software. The averages neural crest cell distribution was quantified and compared between controls and mutants. The average number of dorsal neural crest cells were significantly higher in mutant embryos than controls ($P = 0.034978$).

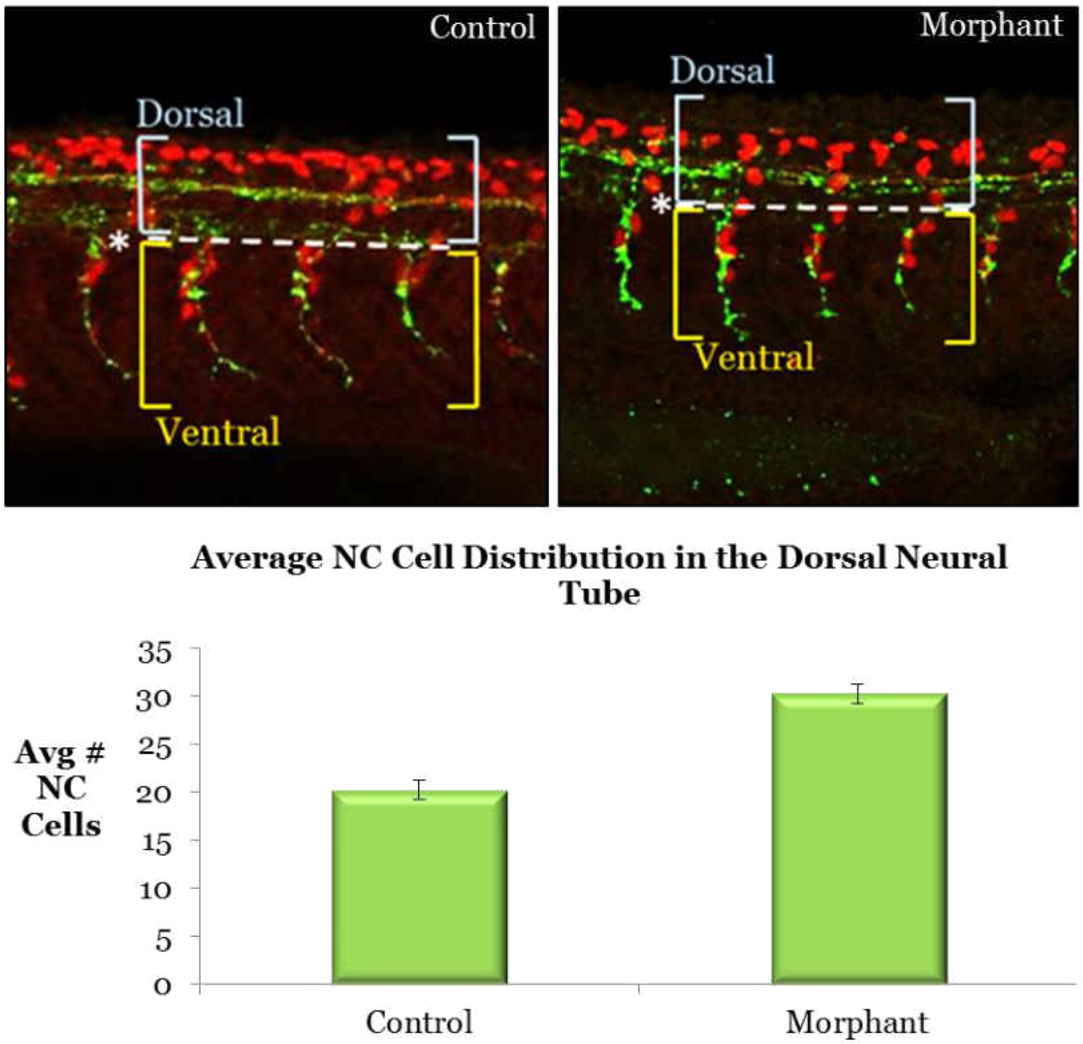

Figure 19. Confocal images of control (Top, Left) and *myo10* MO-injected (Top, Right) ~24hpf zebrafish trunks using znp-1 antibodies fluorescing the primary motor axons in green and sox-10 antibodies fluorescing the neural crest cells in red. * White dashed line represents the bottom of the spinal cord. Neural crest cells above the line were categorized as dorsal neural crest cells. The average number of dorsal neural crest cells were significantly higher in mutant embryos than controls Students T test: P = .034978

4.22 Exogenous *Myo10* Increases CaP Motor Axon Protrusions

Inducing gene overexpression involves exposing an embryo to exogenous mRNA. While gene knockdown is a widely utilized tool to characterize mutations and study molecular mechanisms, gene overexpression is another powerful tool to identify phenotypes and pathways that may have been missed in a typical loss-of-function analysis (Prelich, 2012). Just like gene knock-down, overexpression of a gene in an otherwise wild-type embryo can also cause mutant phenotypes. Figure 20 shows a comparison of control and overexpressed axon and acetylcholine phenotypes. I did not

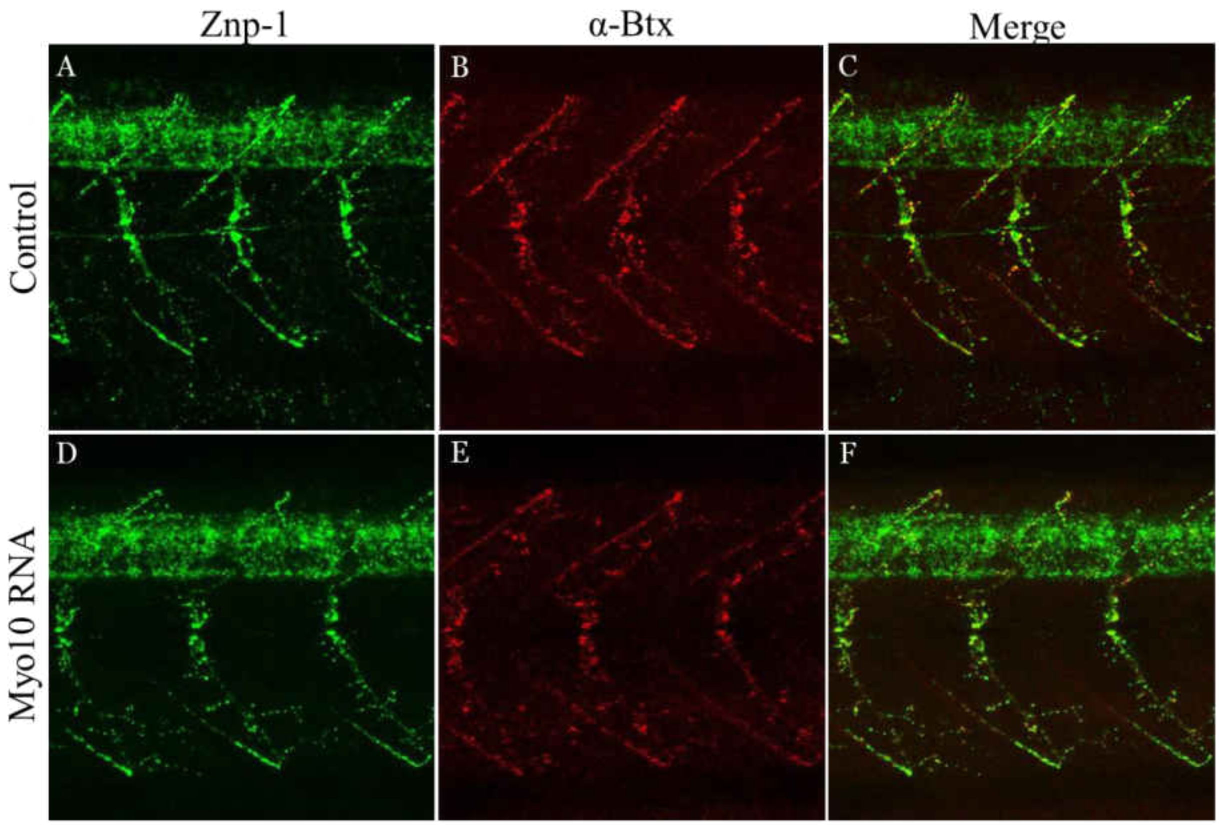

Figure 20. Confocal images of 15^{th}- 17^{th} myotomes of 48 hpf zebrafish trunks fluorescing the CaP motor axons in green with znp-1 antibodies (A and D), the acetylcholine rectors in red with α-Bungarotoxin (B and E), and merged images of the motor axon and α-Bungarotoxin stains (C and F).

detect defects of the CaP or MiP motor axons, nor did the acetylcholine receptors appear disorganized. However, I did detect an increased number of protrusions in overexpressed axons. Figure 21 shows a comparison of control and overexpressed spinal motor axons in the 15^{th} -17^{th} myotome of the zebrafish trunk. Arrowheads were placed to show protrusions in CaP motor axons located on the axon in the center of each picture.

A dashed line was placed underneath the highest intensity, and large mass of neural tissue immediately exiting the spinal cord. Because znp-1 does not differentiate between

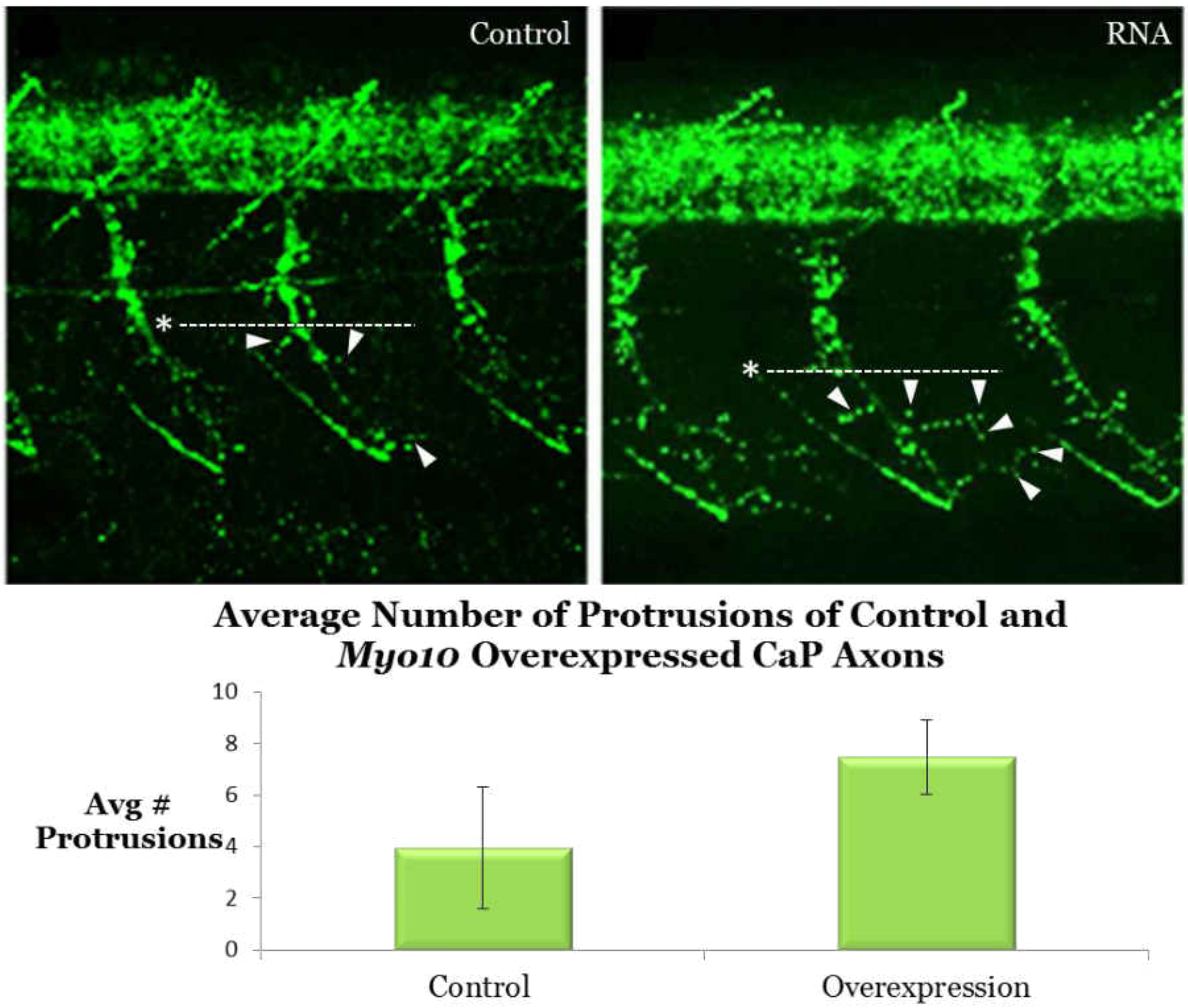

Figure 21. Confocal images of 15th- 17th myotomes of 48 hpf zebrafish trunks fluorescing the CaP motor axons in green with znp-1 antibodies (A and D), the acetylcholine rectors in red with α-Bungarotoxin (B and E), and merged images of the znp-1 and α-Bungarotoxin stains (C and F). G: Summary of the average number of protrusions of control CaP axons compares to CaP axons with *myo10* overexpression Students T test: P<.0001. White arrows indicate protrusions. * Protrusions above dashed line were not counted as CaP protrusions due to possiblity of being RoP protrusions.

the three primary motor axon types, this ensures that protrusions counted are only coming from the CaP motor axon.

4.23 Exogenous *Myo10* Partially Rescues Morphants

MO experiments involve creating a complementary piece of RNA that will successfully hybridize to target mRNA to create a barrier to prevent protein production. It is possible that a MO could generate by-products that could have deleterious effects on development. It is also possible that the MO could be hybridizing to unspecific targets and thus generating a domino effect that could lead to secondary phenotypes not caused directly by a lack of *myo10*. In order to analyse the effectiveness of my MO experiments, I co-injected synthetic *myo10* RNA with *myo10* MO and observed the characteristics of the axons, acetylcholine receptors, and the neural crest cells as described previously. Figure 22 shows the axons in green in the first column, the acetylcholine receptors in red in the second column, and merged images of both the red and green in the last column. As seen in the first row, the control produces normal axon and acetylcholine phenotypes. The second row displays phenotypes associated with the *myo10* mutation. The third row are images of zebrafish embryos that were co-injected with the *myo10* MO and the synthetic *myo10* RNA. When compared to the control, the *myo10* injected morphants have stunted axon growth in approximately 90% of observed axons as shown in Figure 22. The extent of the growth defect varied from severely stunted in such a way that the dorsal curvature seen at the bottom of CaP motor axons was completely missing while some defected CaP axons maintained a portion of this curvature. In order to standardize the data for the purposes of determining the ability of *myo10* to be rescued, I defined a rescued axon to have the dorsal extension that is often missing in morphant CaP motor axons. Individuals displaying defective CaP motor axons consequently also suffer from a severe growth and patterning defect of acetylcholine receptors. Also, MiP motor axons extending dorsally over the spinal cord are also often missing in *myo10* deficient embryos. Figure 22 demonstrates that rescued individuals can regain dorsal curvature of the CaP axon and acetylcholine receptors and an increase in the number of present MiP motor axons.

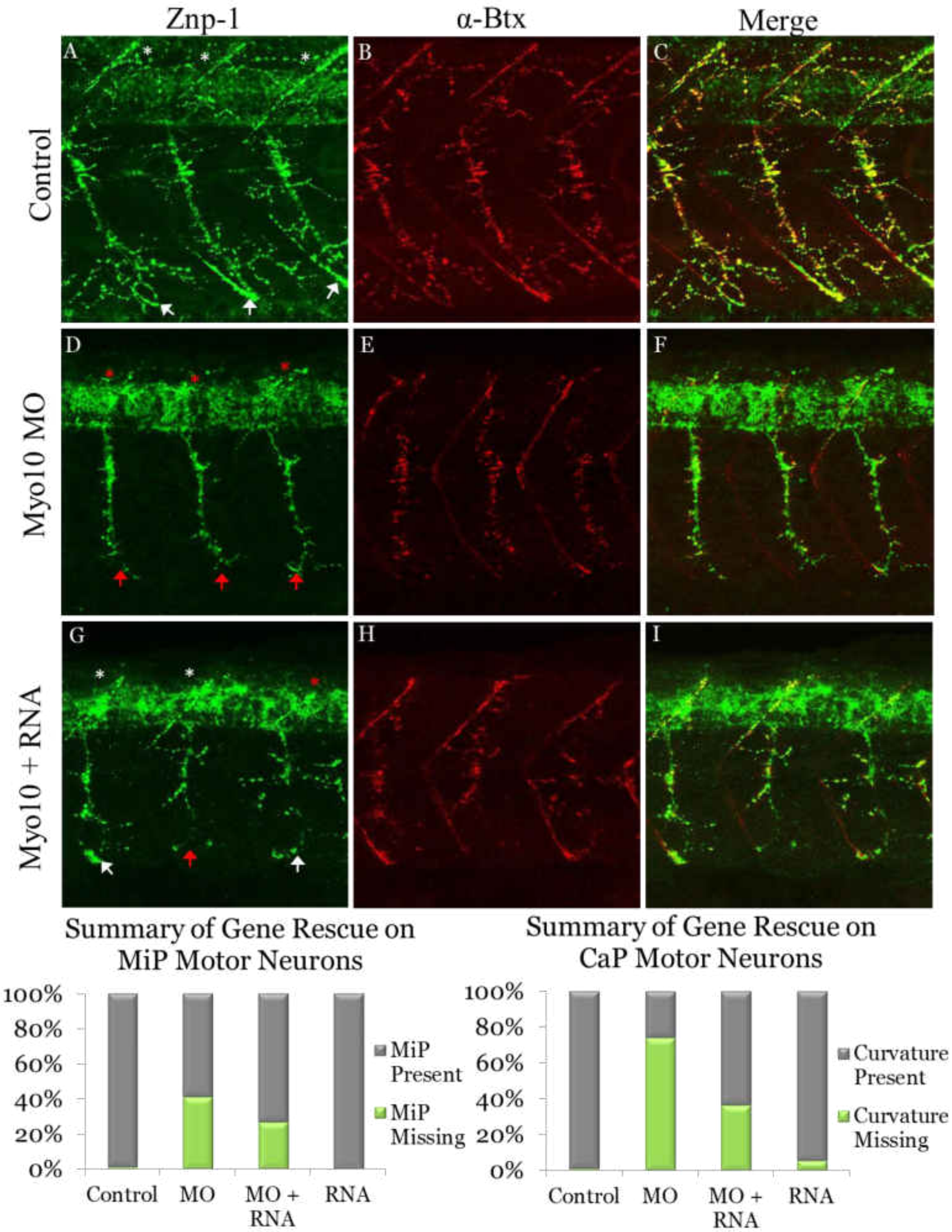

Figure X. Confocal images of 15^{th}- 17^{th} myotomes of 48 hpf zebrafish trunks fluorescing the motor neurons in green with znp-1 antibodies (A, D and G), the acetylcholine rectors in red with α-Bungarotoxin (B, E and H), and merged images of the motor axon and α-Bungarotoxin stains (C, F, and I). Images reveal that co-injection of *myo10* MO with *myo10* RNA partially rescues the phenotype. White astericks indicate present MiP axons. Red Astriks indicate missing MiP axons. White arrows indicate CaP axons with dorsal curvature preent. Red arrows indicate CaP axons that are missing the dorsal curvature.

CHAPTER 5

DISCUSSION

Cell culture data has supplied us with a plethora of information about axon guidance including the four main classes of axon guidance molecules (ephrins, slits, semaphorins, and netrins), their receptors, and their effect on steering the growth cone. Typically, ephrins, slits, and semaphorins are associated with growth cone repulsion, while netrins are associated primarily with attraction (Yu and Bargmann, 2001). While it has also been demonstrated that these molecules can be multi-functional (involved in both attraction and repulsion), I will focus on their typical roles of axon guidance. ephrins bind to eph receptors. In response, the rho family guanine nucleotide exchange factor (GEF), vav2, is recruited. This allows for endocytosis of ephA resulting in growth cone collapse and repulsion (Bashaw and Klein, 2010). Slits bind to robo receptors resulting in growth cone repulsion at the midline to prevent ipsilateral axons from crossing the midline and commissural axons from re-crossing (Dickson et al. 2002). Semaphorins are a very large family of axon guidance molecules that fall into 8 classes and bind to multimeric receptor complexes that result in growth cone repulsion when activated (Dickson et al. 2002) and some have been shown to be involved in motor axon growth and guidance (Huber et al. 2006). Netrins bind to Deleted in Colorectal Cancer (DCC) homodimers, which leads to growth cone attraction by increasing the number of filopodia and surface area of the growth cone (Huber et al. 2003). While these extracellular axon guidance molecules have been extensively studied, little is known about axon pathfinding due to intracellular molecules. Because growth cones of neurons are actin rich, it is likely that intracellular molecules involved in axon guidance are actin binding molecules. Myosins are the only known actin-based motor proteins that are associated in cell motility and therefore are a likely candidate in the regulation of axon growth during development (Hartman and Spudich 2012). Most experimentation regarding *myo10* to date has been performed *in vitro*. While *in vitro* experimentation has given us some insight on how *myo10* functions. Its function will not be fully understood until its mechanisms can be described in the absence of the estimated factors used in *in vitro* studies. *In vivo* experimentation offers further understanding of an experiment on a living system whose molecular dynamics drastically change during embryogenesis. My *in vivo* data has demonstrated that *myo10* is required for proper spinal motor and hindbrain axon growth and guidance. M*yo2* is a similarly structured molecule in the same superfamily as *myo10* (Brown and Bridgman, 2003). *Myo2* has previously been shown to play a role in axon guidance from within the axon. In recent studies, evidence has shown that *myo2* is primarily associated with generation of retrograde flow of actin and contractile forces associates with cell migration in which *myo2* possibly results in "dragging" that poster portion of the growth cone towards the direction of growth (Bridgman et al. 2001). It has been demonstrated that axonal elongation will still occur in the presence of actin polymerizing inhibitors and *myo2*. However, without actin dynamics, axonal elongation is slow and unresponsive to extrinsic cues (Gomez and Letourneau, 2014). Similarly, inhibition of *myo10* still allowed axon elongating but growth was truncated and misguided. Because similar results are observed in knock outs of *myo10*, it is likely that the *myo10* axon phenotype is the result of a defect in *myo10*'s association with actin.

Myo10 is an actin binding molecule that is expressed in both the growth cones of projecting axons and the neural crest cells. Interestingly, others have demonstrated that defects in neural crest cells yields faulty axon growth. Thus, I speculate that it is possible that *myo10* may be functioning within the growth cone of neurons and/or the neural crest cells.

5.1 *Myo10* Could be Functioning within the Growth Cone

Experiments demonstrating expression patterns of *myo10* were performed by Nie et al. (2009) *in vitro* showing that *myo10* localizes to axon growth cone filopodial tips *in vitro*. Another study performed by Yu et al. 2012 used plated rat hippocampal neurons to show that *myo10* shows preferential accumulation of *myo10* to the filopodial tips of axon growth cones. The same study also demonstrated that down regulation of myo10 using mRNA yielded smaller growth cones, less filopodial extensions, a decrease in the longest length of neurite outgrowths, and less axon formation (Yu et al. 2012). These results coincide with my *in vivo* data that shows that both CaP and MiP axons are affected as a results of deficiencies of *myo10*. In Cap Motor axons I saw a consistent truncation of axon growth and MiP motor axons were often missing completely. Additionally, over-expression of *myo10* has been reported to induce filopodial protrusions and to regulate growth cone motility *in vitro* (Watanabe et al. 2010). My results indicate that increasing the expression of *myo10* displays no defect in the zebrafish trunk in regards to truncation of CaP motor axons or missing MiP motor axons which are both phenotypes seen in the gene knockdown. However, wild-type embryos exposed to exogenous *myo10* mRNA have an increased number of protrusions along the CaP motor axons. Because exogenous *myo10* mRNA caused an increase in filopodial protrusions *in vitro*, I speculate that the increase in axon protrusions *in vivo* is also caused by an increase in filopodial protrusions during axon growth.

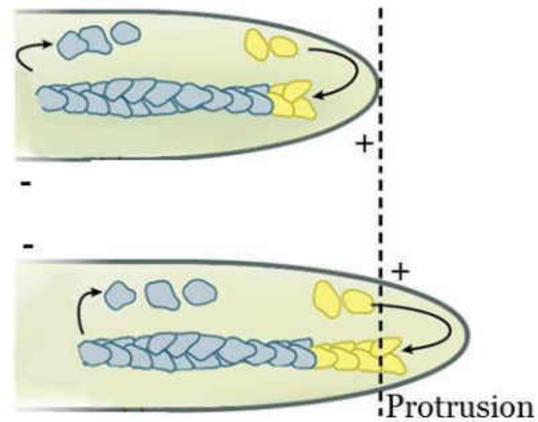

Figure 24. Schematic of actin polymerization in filopdia. Polymers of F-actin (in blue) form filaments that new globular actin (in yellow) add to at the leading edge to form filopodial protrusions. Picture amended from MBInfo contributors.

Because *myo10* in the growth cone filopdia are actin-binding motor proteins, it is likely that *myo10* affects axon elongation and guidance through altering actin dynamics. This occurs as demonstrated in Figure 24 due to actin polymerization that takes place at the leading edge of actin filaments at their plus (barbed) end (Mitchison and Cramer, 1996). During Neural outgrowth, actin-rich filopodia first extend to explore the extracellular matrix (ECM) in search of molecular cues in the extracellular matrix. These cues associate with receptors location on the cell membrane of the growth cone. For example, the axon guidance molecule netrin-1 binds to DCC receptors on the growth cone. This causes a cascade of events that ultimately phosphorylates and activates Ena/Vasp proteins (Lebrand et al. 2004). Interestingly, it has been demonstrated that

Figure 25. Model of Myosin 10's function in filopodia elongation. (A) If capping proteins bind to the plus end of actin filaments, the elongation of actin bundles is blocked. (B) If Myosin 10 transports enough Mena/VASP to the tip of the filopodia to outcompete the capping proteins, the transported VASP promotes actin filament elongation by interacting with the plus ends, shielding them from the capping protein. Picture taken from Tokuo and Ikebe, 2004.

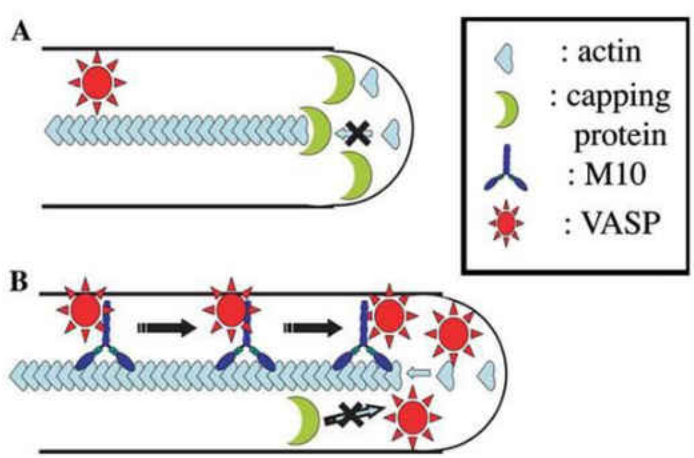

Vasp proteins are a cargo of *myo10*. *Myo10* is believed to be invovled in actin polymerization by utilizing its actin binding motor to "walk" down F-actin fiaments in a step like fasion where it transports cargos (Ricca and Rock, 2010). Hypothesized molecular structures suggests that *myo10* dimerizes to form a molecule whose head domains binds to actin and "walk" along actin filaments at the filopodial tips in a hand-over-hand processive fashion (Ricca and Rock, 2010). In order to activate *myo10*'s capacity to utilize its motor to transport, phosphoinositol PI3-kinase (PI3K) is activated within the filopodia. These kinases generate PtdIns that recruit *myo10* (Isakoff 1998). PtdIns are membrane-anchored lipids that serve as docking sites for many pleckstrin homology domain-containing proteins. *Myo10* contains a PH domain within its tail that can bind ptdIns which enhances *myo10* localization to the filopodia and promotes is motor activity (Arjonen et al. 2011, Plantard 2010 and Yu at al. 2012). Once *myo10* is localized to the filopodia, it can bind Mena/Vasp at its MyTH4/FERM domain and transport it to filopodial tip. This hypothesized mechanism aligns with studies that have deleted the cargo carrying MyTH4/FERM domains which abolished *myo10*'s ability to promote filopodial extension (Wei et al. 2010). VASP proteins inhibit protein capping of actin filaments that allow additional actin polymers to be adding to the bared end of the actin filament (See Figure 24). *Myo10* has been demonstrated to transport Mena/VASP to the filopodial tips in cell cultures (Tokuo and Ikebe, 2004). Taken together, because axons deficient in *myo10* in zebrafish display stunted axon growth, it is likely that *myo10* functions in filopodial extension *in vivo* via transportation of Mena/VASP that is likely bound to the myTH4/FERM complex of *myo10*. Without *myo10*, the Mena/VASP will not be transported to the filopodial tip to compete with capping proteins. Without removal of capping proteins, filopodial extension will not occur. Consequently, the inability of axon elongation results in the observed stunted axon development.

Another possible mechanism behind filopodial growth is that *myo10* transports other cargos such as DCC. Zhu et al. 2007 showed that *myo10* transported DCC to the filopodial tips. This is interesting because DCC interacts with molecules involved in netrin signaling which promotes axon outgrowth and mediates attractive growth cone guidance of axon projections (Liu, 2012).

Others have seen similar defects in morphants that have mutations in other genes. For example, the gene, *diwanka*, has been shown to control growth cone guidance (Zeller and Granato, 1999). In *diwanka* deficient zebrafish embryos, the spinal motor neurons in the trunk are still present, but CaP and Mip motor axons are truncated 95% of the time to some degree. Zeller and Granato also examined hindbrain neurons in *diwanka* mutants and observed no defect. In *myo10* deficient embryos, I observed the same truncation in the CaP and MiP axons. However, I also observed defects in hindbrain axons. Thus, it is likely that both gene products are involved in the same process but in cell populations that *diwanka* is not. *Unplugged* mutants also display spinal motor neuron defects in the trunk of the zebrafish. However this mutation results in a different defect. In *unplugged* mutants, CaP and RoP motor neurons have abnormal axon projections while MiP appears normal (Beattie, 2000). Because I saw a different defect, it is likely that *myo10* and *unplugged* gene products are involved in separate processes. *Stumpy* mutants also display spinal motor axon guidance defects that cause elongation pausing of CaP motor axons during axon elongation (Beattie, 2000). In order to determine if *myo10* is required for axon elongation past intermediate targets like *stumpy*, time-lapse observations of *myo10* deficient axons are necessary. Finally, survival motor neuron (*smn)* also displays defects in the spinal motor axons (McWhorter et al. 2003). At low levels, motor axon branching and truncating was observed. At higher levels, truncation was less common and more branching occurred.

5.2 Muscle Defects are a Result of Motor Neuron Defects

Axon elongation and migration of primary motor axons completes when the growth cone reaches its target, the muscle. The combination of the axon and muscle forms a synapse at the neuromuscular junction. This complex is made of up the pre-synaptic axon and the post synaptic muscle (Wu et al. 2010). The muscle membrane is lined with acetylcholine receptors that are produced in response to Acetylcholine Receptor Inducing Activity (ARIA); a glycoprotein made by motor neurons and released at the neuromuscular synapse to stimulate the synthesis of acetylcholine receptors by skeletal muscle. These receptors bind Acetylcholine which transmits signals across the synapse from the axon to the muscle for contraction (Wu et al. 2010). By labeling the acetylcholine receptors with the axons, I was able to see both the pre-synaptic and post-synaptic ends of the complex to reveal information about neural circuitry. In the morphant, acetylcholine receptors were present, yet unorganized compared to the controls. This means that while synapses were still forming at neuromuscular junctions, they are not forming in the right places. Consistent with this observation, I observed mobility defects in morphant individuals, but not paralysis. Additionally, instead of a streamline flow of seemingly uniformly distributed acetylcholine receptors, the concentration of acetylcholine receptors of morphants appeared upregulated in the areas where they are present, giving them a blotchy labeling in fluorescent labeling. This is consistent with a study done in chick that demonstrated that muscle denervation activates acetylcholine receptor genes (Tsay and Schmidt, 1989). Because issues with synapses often lead to muscle defects in neurodegenerative diseases, I examined the muscles. I observed the slow muscle bands and did not see a difference in band numbers across all groups (control, MO-injected, and RNA-injected). However, the thickness of the bands were significantly smaller in MO-injected embryos compared to controls ($P<.0001$). Others have demonstrated that denervation of the muscular tissue from the nervous system results in muscle fibers thickness decrease in rat indicating muscular atrophy (Fambrough, 1974). Thus, the decrease in myofibril width indicates muscular atrophy which is likely to be a causal effect from the synaptic defects. The disorganized distribution of acetylcholine patterns is indicative of improper innervation of the muscles from the axons. In many neurodegenerative diseases such as muscular dystrophy and Amyotrophic Lateral Sclerosis (ALS) axons loose connectivity with the muscles. This lack of connectivity leads to muscle weakness and eventually degeneration (Fambrough, 1974). A related disease, Spinal Muscular Atrophy (SMA) has been associated with loss of *smn* protein previously mentioned (Winkler et al. 2005). In the previous study by McWhorter et al. 2003, they observed muscle cross sections of *smn* mutants and reported not to see any defect in the muscle. However, I observed lateral images of zebrafish *myo10* mutants displaying similar axon phenotypes in the axons that were seen in *smn* mutants. Axon truncations observed resulted in musculature innervation disorganization. Because innervation is induced by the neurons themselves and not the muscle (Corfas, 1992), it is probably that *smn* mutants also have disorganized acetylcholine receptors. The acetylcholine receptor mispatterning indicates musculature innervation defects which have been shown to cause muscle band thickness decreases and result in the muscular atrophy seen. While this is only speculation, a more recent study observed muscle fiber areas in control and *smn* deficient rats. They reported that while there was no difference in muscle fiber counts or muscle fiber area means, there was a difference in distribution of muscle fiber are between *smn* mutants and controls (Gavrilina et al. 2007).

In zebrafish, there are three *myo10* genes; *myo10a*, *myo10b*, and *myo10c*. *Myo10a* has been shown to be present in the spinal cord and developing neurons at 18hpf along with other areas in the brain at 30hpf (Sittaramane and Chandrasekhar, 2008). While expression patterns of *myo10b* and *myo10c* are still unknown, leaving the possibility that *myo10* defects are due to a down regulation of *myo10* functioning in the muscle, it is likely that muscle band width defects are a causal effect from muscle weakening due to innervation issues instead of a direct effect of *myo10* knockdown. Muscle weakness is typical in patients with neuromuscular disorders such as muscular dystrophy and Amyotrophic Lateral Sclerosis (ALS) in humans. Interestingly, it has been recorded that primary motor neurons in zebrafish form synapses with fast muscle fibers and not slow muscle fibers. Instead, secondary motor neurons (smn) form synapses with the slow muscle fibers (Babin et al. 2014). Thus, *myo10* deficiencies may also cause snm defects that are causing the slow muscle malformation. Future experiments should be performed that examine smn with slow *myo10* deficient individuals as well as experiments examining the primary motor axons in conjunction with fast muscle tissue.

5.3 *Myo10* may be functioning in Neural Crest Cells

In the second phase of neural outgrowth described previously, filopodia adhere to the substrate in response to attractive molecules via complex interactions between extracellular matrix proteins, cell adhesion proteins, and the actin cytoskeleton. *Myo10* has been shown to form complexes with integrins which are cell adhesion proteins that bind to its FERM domain and possibly serve as a link between actin filaments and the extracellular (Arjonen et al. 2011 and Breshears et al. 2010). However, Hirano et al. claims that DCC binding of *myo10* interferes with integrin binding. Because DCC bound to *myo10* induces netrin signaling and thus axon outgrowth, it is possible that another molecule interacts with integrins to support adhesive contacts with the ECM or that DCC and integrins compete for *myo10* thus allowing for both adhesion and extension simultaneously. Knowing that *myo10* is capable of linking actin inside the filopodia to the outside of the cell makes is possible that this property could allow *myo10* to serve as a link between the filopodia and the neural crest cells. It is possible that the filopodia essentially use the migrating neural crest cells in the vicinity as a tool to help generate new focal points.

Another gene that has been associated with neural crest cell specification and migration is *foxd3*. *Sym-1* mutants have a deletion that disrupts the DNA binding domain of the *foxd3* gene. At 24hpf, control zebrafish embryos expressing sox 10 (a neural crest cell marker) showed normal stream-like migration patterns in the trunk (Stewart et al. 2005). However, s*ym-1* mutant sox-10 expressing cells were still on the dorsal neural tube. This coincides with my data in *myo10* mutant individuals where sox-10 expressing cells are present but migration appears to be arrested. Other molecules involved in proper neural crest cell migration are MuSK and Wnt11r. In deficient embryos, neural crest cells still migrate, but are not restricted to the typical organized streams that follow spinal motor axons in control embryos (Banerjee et al. 2011).

5.4 Future Directions

While I have provided a lot of information on the morphology of myo10 deficient embryos, there is a lot to test to determine how *myo10* functions. I observed the commissural axons in the hindbrain to test the specificity of *myo10*. These axons also express *myo10* during development. In the morphant, the commissural axons fail to migrate. So far, tissue expressing *myo10* has displayed defects. This indicates that *myo10* is likely to be specific to its expression pattern. However, further experiments must be done in tissues that do not express *myo10*. If tissues that do not express myo10 form normally, then *myo10* can be reported to function specifically.

Because, myo10 protein is an intracellular protein and is unable to travel across cell membranes, I could determine if *myo10* is functioning within the axons by a series of transplantation experiments. Transplantation techniques can be used to create genetic mosaic organisms known as chimeras that allow a mixture of cells of two or more different genotypes to be incorporated into a single organism (Carmany-Rampey, 2006). This method enables us to analyse mutant cells in an otherwise wildtype environment and vice versa. Others have also used this technique to successfully identify the cell autonomy of other genes such as spt-1 (Ho and Kane, 1990). Additionally, Song et al. 2013 successfully utilized transplantation of zebrafish spinal motor neurons. Completing a series of transplant experiments in both neurons and neural crest cells will help deduce where *myo10* in functioning *in vivo*.

No rescue experiments of *myo10* defect have previously been done. My *in vivo g*ene rescue experiments shows that there is a possibility to rescue axon phenotypes by co-injecting *myo10* MO knock down embryos with exogenous *myo10* mRNA. Knock-down embryos display severely truncated CaP motor axons in which ~74% do not migrate ventrally after dorsal elongation. Co-injection of exogenous *myo10* mRNA with the *myo10* MO resulted in ~36% of axons missing the ventral curvature. While the rescue seemed to increase the CaP motor axons ability to elongate, axons were still not completely rescued. They appear to by misguided rosto-causally, while still maintaining the stereotypical ventral elongation followed by a dorsal curvature. Replacement of endogenous protein with exogenous proteins can cause a lot of problems *in vivo*. For example, introducing a large volume of exogenous material can be toxic to a developing embryo. This can affect the overall health of the organism and could explain the results. Partial rescue after co-injection of a MO with mRNA is commonly in other rescues (McWhorter et al. 2003 and McClintock 2002) and is probably caused by the mosaicism of RNA distribution. After co-injecting of *myo10* MO and *myo10* RNA *in vivo,* the experimenter has no control of how these particles diffuse. It is possible that exogenous amounts of mRNA and the MO are not equally distributed throughout the embryo.

References

Ananthakrishnan R, Ehrlicher A. 2007. The forces behind cell movement. International Journal of Biological Sciences 3:303-317.

Arjonen A, Kaukonen R, Ivaska J. 2011. Filopodia and adhesion in cancer cell motility. Cell Adhesion & Migration 5:421-430.

Aviles EC, Wilson NH, Stoeckli ET. 2013. Sonic hedgehog and Wnt: antagonists in morphogenesis but collaborators in axon guidance. Frontiers in Cellular Neuroscience 7.

Babin PJ, Goizet C, Raldua D. 2014. Zebrafish models of human motor neuron diseases: Advantages and limitations. Progress in Neurobiology 118:36-58.

Banerjee S, Gordon L, Donn TM, Berti C, Moens CB, Burden SJ, Granato M. 2011. A novel role for MuSK and non-canonical Wnt signaling during segmental neural crest cell migration. DEVELOPMENT -CAMBRIDGE- 138:3287-3296.

Banerjee S, Isaacman-Beck J, Schneider VA, Granato M. 2013. A Novel Role for Lh3 Dependent ECM Modifications during Neural Crest Cell Migration in Zebrafish. Plos One 8.

Bashaw GJ, Klein R. 2010. Signaling from Axon Guidance Receptors. Cold Spring Harbor Perspectives in Biology 2.

Bassett D, Currie PD. 2004. Identification of a zebrafish model of muscular dystrophy. Clinical and Experimental Pharmacology and Physiology 31:537-540.

Bassett DI, Currie PD. 2003. The zebrafish as a model for muscular dystrophy and congenital myopathy. Human Molecular Genetics 12:R265-R270.

Bastida MF, Sheth R, Ros MA. 2009. A BMP-Shh negative-feedback loop restricts Shh expression during limb development. Development 136:3779-3789.

Berg JS, Cheney RE. 2002. Myosin-X is an unconventional myosin that undergoes intrafilopodial motility. Nature Cell Biology 4:246-250.

Betz T, Koch D, Lim D, Kaes JA. 2009. Stochastic Actin Polymerization and Steady Retrograde Flow Determine Growth Cone Advancement. Biophysical Journal 96:5130-5138.

Bill BR, Petzold AM, Clark KJ, Schimmenti LA, Ekker SC. 2009. A Primer for Morpholino Use in Zebrafish. Zebrafish 6:69-77.

Breshears LM, Wessels D, Soll DR, Titus MA. 2010. An unconventional myosin required for cell polarization and chemotaxis. Proceedings of the National Academy of Sciences of the United States of America 107:6918-6923.

Bridgman PC, Dave S, Asnes CF, Tullio AN, Adelstein RS. 2001. Myosin IIB is required for growth cone motility. Journal of Neuroscience 21:6159-6169.

Bronnerfraser M. 1994. NEURAL CREST CELL-FORMATION AND MIGRATION IN THE DEVELOPING EMBRYO. Faseb Journal 8:699-706.

Brown J, Bridgman PC. 2003. Role of myosin II in axon outgrowth. Journal of Histochemistry & Cytochemistry 51:421-428.

Carmany-Rampey A, Moens CB. 2006. Modern mosaic analysis in the zebrafish. Methods 39:228-238.

Chapleau C, Lane J, Pozzo-Miller L, Percy A. 2013. Rett Syndrome: A Model of Genetic Neurodevelopmental Disorders. In: InTech, 2013-01-09.

Charron F, Tessier-Lavigne M. 2007. The Hedgehog, TGF-beta/BMP and Wnt families of morphogens in axon guidance. Axon Growth and Guidance 621:116-133.

Corfas G, Falls DL, Fischbach GD. 1993. ARIA, A PROTEIN THAT STIMULATES ACETYLCHOLINE-RECEPTOR SYNTHESIS, ALSO INDUCES TYROSINE PHOSPHORYLATION OF A 185-KDA MUSCLE TRANSMEMBRANE PROTEIN. Proceedings of the National Academy of Sciences of the United States of America 90:1624-1628.

Dent EW, Gupton SL, Gertler FB. 2011. How the growth cone moves during axon outgrowth and guidance. Cold Spring Harb Perspect Biol 3: a001800.

Dent EW, Gupton SL, Gertler FB. 2011. The growth cone cytoskeleton in axon outgrowth and guidance. Cold Spring Harbor perspectives in biology 3.

Dickson BJ. 2002. Molecular mechanisms of axon guidance. Science 298:1959-1964.

Ehninger D, Li W, Fox K, Stryker MP, Silva AJ. 2008. Reversing Neurodevelopmental Disorders in Adults. Neuron 60:950-960.

Eisen JS. 1991. DEVELOPMENTAL NEUROBIOLOGY OF THE ZEBRAFISH. Journal of Neuroscience 11:311-317.

Fambroug.Dm. 1974. ACETYLCHOLINE RECEPTORS - REVISED ESTIMATES OF EXTRAJUNCTIONAL RECEPTOR DENSITY IN DENERVATED RAT DIAPHRAGM. Journal of General Physiology 64:468-472.

Flanagan-Steet H, Fox MA, Meyer D, Sanes JR. 2005. Neuromuscular synapses can form in vivo by incorporation of initially aneural postsynaptic specializations. Development 132:4471-4481.

Gavrilina TO, McGovern VL, Workman E, Crawford TO, Gogliotti RG, DiDonato CJ, Monani UR, Morris GE, Burghes AHM. 2008. Neuronal SMN expression corrects spinal muscular atrophy in severe SMA mice while muscle-specific SMN expression has no phenotypic effect. Human Molecular Genetics 17:1063-1075.

Gilbert SF. 1997. Developmental biology. Fifth edition. Developmental biology. Fifth edition.:i-xix, 1-918, Q.911, AI.911-AI.913, SI.911-SI.925.

Gomez TM, Letourneau PC. 2014. Actin dynamics in growth cone motility and navigation. Journal of Neurochemistry 129:221-234.

Guthrie S. 2007. Patterning and axon guidance of cranial motor neurons. Nature Reviews Neuroscience 8:859-871.

Hammerschmidt M, Wedlich D. 2008. Regulated adhesion as a driving force of gastrulation movements. Development 135:3625-3641.

Hartman MA, Spudich JA. 2012. The myosin superfamily at a glance. Journal of Cell Science 125:1627-1632.

Hasson T, Skowron JF, Gilbert DJ, Avraham KB, Perry WL, Bement WM, Anderson BL, Sherr EH, Chen ZY, Greene LA, Ward DC, Corey DP, Mooseker MS, Copeland NG, Jenkins NA. 1996. Mapping of unconventional myosins in mouse and human. Genomics 36:431-439.

Heisenberg CP, Tada M, Rauch GJ, Saude L, Concha ML, Geisler R, Stemple DL, Smith JC, Wilson SW. 2000. Silberblick/Wnt11 mediates convergent extension movements during zebrafish gastrulation. Nature 405:76-81.

Hirano Y, Hatano T, Takahashi A, Toriyama M, Inagaki N, Hakoshima T. 2011. Structural basis of cargo recognition by the myosin-X MyTH4-FERM domain. Embo Journal 30:2734-2747.

Hirokawa N, Niwa S, Tanaka Y. 2010. Molecular Motors in Neurons: Transport Mechanisms and Roles in Brain Function, Development, and Disease. Neuron 68:610-638.

Ho RK, Kane DA. 1990. Cell-autonomous action of zebrafish spt-1 mutation in specific mesodermal precursors. Nature:728.

Howe K, Clark MD, Torroja CF, Torrance J, Berthelot C, Muffato M, Collins JE, Humphray S, McLaren K, Matthews L, McLaren S, Sealy I, Caccamo M, Churcher C, Scott C, Barrett JC, Koch R, Rauch G-J, White S, Chow W, Kilian B, Quintais

LT, Guerra-Assuncao JA, Zhou Y, Gu Y, Yen J, Vogel J-H, Eyre T, Redmond S, Banerjee R, Chi J, Fu B, Langley E, Maguire SF, Laird GK, Lloyd D, Kenyon E, Donaldson S, Sehra H, Almeida-King J, Loveland J, Trevanion S, Jones M, Quail M, Willey D, Hunt A, Burton J, Sims S, McLay K, Plumb B, Davis J, Clee C, Oliver K, Clark R, Riddle C, Eliott D, Threadgold G, Harden G, Ware D, Mortimer B, Kerry G, Heath P, Phillimore B, Tracey A, Corby N, Dunn M, Johnson C, Wood J, Clark S, Pelan S, Griffiths G, Smith M, Glithero R, Howden P, Barker N, Stevens C, Harley J, Holt K, Panagiotidis G, Lovell J, Beasley H, Henderson C, Gordon D, Auger K, Wright D, Collins J, Raisen C, Dyer L, Leung K, Robertson L, Ambridge K, Leongamornlert D, McGuire S, Gilderthorp R, Griffiths C, Manthravadi D, Nichol S, Barker G, Whitehead S, Kay M, Brown J, Murnane C, Gray E, Humphries M, Sycamore N, Barker D, Saunders D, Wallis J, Babbage A, Hammond S, Mashreghi-Mohammadi M, Barr L, Martin S, Wray P, Ellington A, Matthews N, Ellwood M, Woodmansey R, Clark G, Cooper J, Tromans A, Grafham D, Skuce C, Pandian R, Andrews R, Harrison E, Kimberley A, Garnett J, Fosker N, Hall R, Garner P, Kelly D, Bird C, Palmer S, Gehring I, Berger A, Dooley CM, Ersan-Ueruen Z, Eser C, Geiger H, Geisler M, Karotki L, Kirn A, Konantz J, Konantz M, Oberlaender M, Rudolph-Geiger S, Teucke M, Osoegawa K, Zhu B, Rapp A, Widaa S, Langford C, Yang F, Carter NP, Harrow J, Ning Z, Herrero J, Searle SMJ, Enright A, Geisler R, Plasterk RHA, Lee C, Westerfield M, de Jong PJ, Zon LI, Postlethwait JH, Nuesslein-Volhard C, Hubbard TJP, Crollius HR, Rogers J, Stemple DL. 2013. The zebrafish reference genome sequence and its relationship to the human genome. Nature 496:498-503.

Huang Y, Wang X, Wang X, Xu M, Liu M, Liu D. 2013. Nonmuscle myosin II-B (myh10) expression analysis during zebrafish embryonic development. Gene Expression Patterns 13:265-270.

Huber AB, Kania A, Tran TS, Gu CH, Garcia ND, Lieberam I, Johnson D, Jessell TM, Ginty DD, Kolodkin AL. 2005. Distinct roles for secreted semaphorin signaling in spinal motor axon guidance. Neuron 48:949-964.

Huber AB, Kolodkin AL, Ginty DD, Cloutier JF. 2003. Signaling at the growth cone: Ligand-receptor complexes and the control of axon growth and guidance. Annual Review of Neuroscience 26:509-563.

Hwang Y-S, Luo T, Xu Y, Sargent TD. 2009. Myosin-X Is Required for Cranial Neural Crest Cell Migration in Xenopus laevis. Developmental Dynamics 238:2522-2529.

Isakoff SJ, Cardozo T, Andreev J, Li Z, Ferguson KM, Abagyan R, Lemmon MA, Aronheim A, Skolnik EY. 1998. Identification and analysis of PH domain-containing targets of phosphatidylinositol 3-kinase using a novel in vivo assay in yeast. Embo Journal 17:5374-5387.

Jessell TM. 2000. Neuronal specification in the spinal cord: Inductive signals and transcriptional codes. Nature Reviews Genetics 1:20-29.

Jung H, O'Hare CM, Holt CE. 2011. Translational regulation in growth cones. Current Opinion in Genetics & Development 21:458-464.

Kerber ML, Cheney RE. 2011. Myosin-X: a MyTH-FERM myosin at the tips of filopodia. Journal of Cell Science 124:3733-3741.

Kettleborough RNW, Busch-Nentwich EM, Harvey SA, Dooley CM, de Bruijn E, van Eeden F, Sealy I, White RJ, Herd C, Nijman IJ, Fenyes F, Mehroke S, Scahill C, Gibbons R, Wali N, Carruthers S, Hall A, Yen J, Cuppen E, Stemple DL. 2013. A systematic genome-wide analysis of zebrafish protein-coding gene function. Nature 496:494-+.

Kimmel CB, Ballard WW, Kimmel SR, Ullmann B, Schilling TF. 1995. STAGES OF EMBRYONIC-DEVELOPMENT OF THE ZEBRAFISH. Developmental Dynamics 203:253-310.

Ko S-K, Chen X, Yoon J, Shin I. 2011. Zebrafish as a good vertebrate model for molecular imaging using fluorescent probes. Chemical Society Reviews 40:2120-2130.

Krendel M, Mooseker MS. 2005. Myosins: Tails (and heads) of functional diversity. Physiology 20:239-251.

Lebrand C, Dent EW, Strasser GA, Lanier LM, Krause M, Svitkina TM, Borisy GG, Gertler FB. 2004. Critical role of Ena/VASP proteins for filopodia formation in neurons and in function downstream of netrin-1. Neuron 42:37-49.

Li P, White RM, Zon LI. 2011. Transplantation in Zebrafish. Zebrafish: Disease Models and Chemical Screens, 3rd Edition 105:403-417.

Liu Y, Peng Y, Dai P-G, Du Q-S, Mei L, Xiong W-C. 2012. Differential regulation of myosin X movements by its cargos, DCC and neogenin. Journal of Cell Science 125:751-762.

Lowery LA, Van Vactor D. 2009. The trip of the tip: understanding the growth cone machinery. Nature Reviews Molecular Cell Biology 10:332-343.

Lu Q, Ye F, Wei Z, Wen Z, Zhang M. 2012. Antiparallel coiled-coil-mediated dimerization of myosin X. Proceedings of the National Academy of Sciences of the United States of America 109:17388-17393.

Mayor R, Theveneau E. 2013. The neural crest. Development 140:2247-2251.

MBInfo contributors. Adhesion influences filopodia protrusion. In MBInfo Wiki, Retrieved 10/21/2014 from http://www.mechanobio.info/figure/figure/1385531423816.jpg.html

McClintock JM, Kheirbek MA, Prince VE. 2002. Knockdown of duplicated zebrafish hoxb1 genes reveals distinct roles in hindbrain patterning and a novel mechanism of duplicate gene retention. Development 129:2339-2354.

McWhorter ML, Monani UR, Burghes AHM, Beattie CE. 2003a. Knockdown of the survival motor neuron (Smn) protein in zebrafish causes defects in motor axon outgrowth and pathfinding. Journal of Cell Biology 162:919-931.

McWhorter ML, Monani UR, Burghes AHM, Beattie CE. 2003b. Knockdown of the survival motor neuron (Smn) protein in zebrafish causes defects in motor axon outgrowth and pathfinding. Journal of Cell Biology 162:919-931.

Mermall V, Post PL, Mooseker MS. 1998. Unconventional myosins in cell movement, membrane traffic, and signal transduction. Science 279:527-533.

Mitchison TJ, Cramer LP. 1996. Actin-based cell motility and cell locomotion. Cell 84:371-379.

Mizuno T, Shinya M, Takeda H. 1999. Cell and tissue transplantation in zebrafish embryos. Molecular Methods in Developmental Biology 127:15-28.

Nandadasa S, Tao Q, Menon NR, Heasman J, Wylie C. 2009. N- and E-cadherins in Xenopus are specifically required in the neural and non-neural ectoderm, respectively, for F-actin assembly and morphogenetic movements. Development 136:1327-1338.

National Institutes of Health (NIH), "Motor Neuron Diseases Fact Sheet," National Institute of Neurological Disorders and Stroke (NINDS). March 2012. NIH Publication No. 12-5371

Nie S, Kee Y, Bronner-Fraser M. 2009. Myosin-X is critical for migratory ability of Xenopus cranial neural crest cells. Developmental Biology 335:132-142.

Pike SH, Eisen JS. 1990. Identified primary motoneurons in embryonic zebrafish select appropriate pathways in the absence of other primary motoneurons. The Journal Of Neuroscience: The Official Journal Of The Society For Neuroscience 10:44-49.

Plantard L, Arjonen A, Lock JG, Nurani G, Ivaska J, Stromblad S. 2010. PtdIns(3,4,5)P-3 is a regulator of myosin-X localization and filopodia formation. Journal of Cell Science 123:3525-3534.

Plazas PV, Nicol X, Spitzer NC. 2013. Activity-dependent competition regulates motor neuron axon pathfinding via PlexinA3. Proceedings of the National Academy of Sciences of the United States of America 110:1524-1529.

Prokop A, Beaven R, Qu Y, Sanchez-Soriano N. 2013. Using fly genetics to dissect the cytoskeletal machinery of neurons during axonal growth and maintenance. Journal of Cell Science 126:2331-2341.

Ricca BL, Rock RS. 2010. The Stepping Pattern of Myosin X Is Adapted for Processive Motility on Bundled Actin. Biophysical Journal 99:1818-1826.

Riley BB, Chiang MY, Storch EM, Heck R, Buckles GR, Lekven AC. 2004. Rhombomere boundaries are Wnt signaling centers that regulate metameric patterning in the zebrafish hindbrain. Developmental Dynamics 231:278-291.

Roche FK, Marsick BM, Letourneau PC. 2009. Protein synthesis in distal axons is not required for growth cone responses to guidance cues. The Journal Of Neuroscience: The Official Journal Of The Society For Neuroscience 29:638-652.

Schmidt R, Straehle U, Scholpp S. 2013. Neurogenesis in zebrafish - from embryo to adult. Neural Development 8.

Sellers JR. 2000. Myosins: a diverse superfamily. Biochimica Et Biophysica Acta-Molecular Cell Research 1496:3-22.

Sittaramane V, Chandrasekhar A. 2008. Expression of unconventional myosin genes during neuronal development in zebrafish. Gene Expression Patterns 8:161-170.

Song Y, Wang M, Mao F, Shao M, Zhao B, Song Z, Shao C, Gong Y. 2013. Knockdown of Pnpla6 protein results in motor neuron defects in zebrafish. Disease Models & Mechanisms 6:404-413.

Stewart RA, Arduini BL, Berghmans S, George RE, Kanki JP, Henion PD, Look AT. 2006. Zebrafish foxd3 is selectively required for neural crest specification, migration and survival. Developmental Biology 292:174-188.

Summerton J, Weller D. 1997. Morpholino antisense oligomers: Design, preparation, and properties. Antisense & Nucleic Acid Drug Development 7:187-195.

Szpir M. 2006. New thinking on neurodevelopment. Environmental Health Perspectives 114:A100-A107.

TessierLavigne M, Goodman CS. 1996. The molecular biology of axon guidance. Science 274:1123-1133.

Tokuo H, Ikebe M. 2004. Myosin X transports Mena/VASP to the tip of filopodia. Biochemical and Biophysical Research Communications 319:214-220.

Tsay HJ, Schmidt J. 1989. SKELETAL-MUSCLE DENERVATION ACTIVATES ACETYLCHOLINE-RECEPTOR GENES. Journal of Cell Biology 108:1523-1526.

Umeki N, Jung HS, Sakai T, Sato O, Ikebe R, Ikebe M. 2011. Phospholipid-dependent regulation of the motor activity of myosin X. Nature Structural & Molecular Biology 18:783-U755.

Wang M, Wen H, Brehm P. 2008. Function of neuromuscular synapses in the zebrafish choline-acetyltransferase mutant bajan. Journal of Neurophysiology 100:1995-2004.

Watanabe TM, Tokuo H, Gonda K, Higuchi H, Ikebe M. 2010. Myosin-X Induces Filopodia by Multiple Elongation Mechanism. Journal of Biological Chemistry 285:19605-19614.

Wei Z, Yan J, Lu Q, Pan L, Zhang M. 2011. Cargo recognition mechanism of myosin X revealed by the structure of its tail MyTH4-FERM tandem in complex with the DCC P3 domain. Proceedings of the National Academy of Sciences of the United States of America 108:3572-3577.

Westerfield M. 2000. The zebrafish book : a guide for the laboratory use of zebrafish (Danio rerio) / Monte Westerfield. [Eugene, Or.] : M. Westerfield, [c2000]Ed. 4.

WHO (2007) Global burden of neurological disorders: Estimates and projections. Neurological disorders. public health challenges (pp. 32) World Health Organization.

Winckler B, Mellman I. 2010. Trafficking Guidance Receptors. Cold Spring Harbor Perspectives in Biology 2.

Wu H, Xiong WC, Mei L. 2010. To build a synapse: signaling pathways in neuromuscular junction assembly. Development 137:1017-1033.

Yu H, Wang N, Ju X, Yang Y, Sun D, Lai M, Cui L, Sheikh MA, Zhang J, Wang X, Zhu X. 2012. PtdIns (3,4,5) P3 Recruitment of Myo10 Is Essential for Axon Development. Plos One 7.

Yu TW, Bargmann CI. 2001. Dynamic regulation of axon guidance. Nature Neuroscience 4:1169-1176.

Zhang HQ, Berg JS, Li ZL, Wang YL, Lang P, Sousa AD, Bhaskar A, Cheney RE, Stromblad S. 2004. Myosin-X provides a motor-based link between integrins and the cytoskeleton. Nature Cell Biology 6:523-531.

Zhu X-J, Wang C-Z, Dai P-G, Xie Y, Song N-N, Liu Y, Du Q-S, Mei L, Ding Y-Q, Xiong W-C. 2007. Myosin X regulates netrin receptors and functions in axonal path-finding. Nature Cell Biology 9:184-U179.